

Journal Pre-proofs

Synthesis and discovery of ω -3 polyunsaturated fatty acid- alkanolamine (PUFA-AA) derivatives as anti-inflammatory agents targeting Nur77

Hua Fang, Jianyu Zhang, Mingtao Ao, Fengming He, Weizhu Chen, Yuqing Qian, Yuxiang Zhang, Yang Xu, Meijuan Fang

PII: S0045-2068(20)31754-5
DOI: <https://doi.org/10.1016/j.bioorg.2020.104456>
Reference: YBIOO 104456

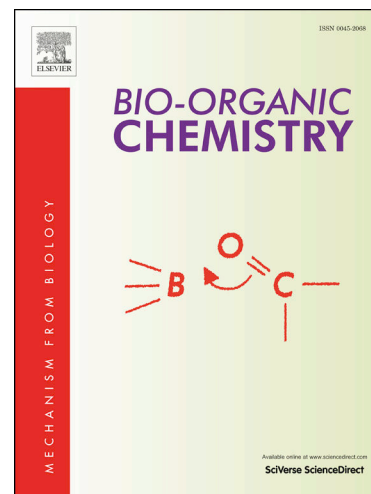
To appear in: *Bioorganic Chemistry*

Received Date: 22 July 2020
Revised Date: 7 September 2020
Accepted Date: 1 November 2020

Please cite this article as: H. Fang, J. Zhang, M. Ao, F. He, W. Chen, Y. Qian, Y. Zhang, Y. Xu, M. Fang, Synthesis and discovery of ω -3 polyunsaturated fatty acid- alkanolamine (PUFA-AA) derivatives as anti-inflammatory agents targeting Nur77, *Bioorganic Chemistry* (2020), doi: <https://doi.org/10.1016/j.bioorg.2020.104456>

This is a PDF file of an article that has undergone enhancements after acceptance, such as the addition of a cover page and metadata, and formatting for readability, but it is not yet the definitive version of record. This version will undergo additional copyediting, typesetting and review before it is published in its final form, but we are providing this version to give early visibility of the article. Please note that, during the production process, errors may be discovered which could affect the content, and all legal disclaimers that apply to the journal pertain.

© 2020 Published by Elsevier Inc.



Synthesis and discovery of ω -3 polyunsaturated fatty acid-alkanolamine (PUFA-AA) derivatives as anti-inflammatory agents targeting Nur77

*Hua Fang^{a,#}, Jianyu Zhang^{b,#}, Mingtao Ao^b, Fengming He^b, Weizhu Chen^a, Yuqing Qian^b, Yuxiang Zhang^b, Yang Xu^{b,**}, Meijuan Fang^{b,*}*

^a Third Institute of Oceanography, Ministry of Natural Resources, Technical Innovation Center for Utilization of Marine Biological Resources, Ministry of Natural Resources, Xiamen, 361005, China.

^b Fujian Provincial Key Laboratory of Innovative Drug Target Research and State Key Laboratory of Cellular Stress Biology, School of Pharmaceutical Sciences, Xiamen University, Xiamen 361102, China.

[#]These authors contributed equally to this paper.

*Corresponding author: Meijuan Fang, School of Pharmaceutical Sciences, Xiamen University, South Xiang-An Road, Xiamen, 361102, China. Phone: +86-592-2189868; Fax: +86-592-2189868. Email: fangmj@xmu.edu.cn.

**Corresponding author: Yang Xu, School of Pharmaceutical Sciences, Xiamen University, South Xiang-An Road, Xiamen, 361102, China. Phone: +86-592-2189868; Fax: +86-592-2189868. Email: xu_yang@xmu.edu.cn.

**Synthesis and discovery of ω -3 polyunsaturated fatty acid-
alkanolamine (PUFA-AA) derivatives as anti-inflammatory
agents targeting Nur77**

Hua Fang^{a,#}, Jianyu Zhang^{b,#}, Mingtao Ao^b, Fengming He^b, Weizhu Chen^a, Yuqing Qian^b, Yuxiang Zhang^b, Yang Xu^{b,*}, Meijuan Fang^{b,*}

^a Third Institute of Oceanography, Ministry of Natural Resources, Technical Innovation Center for Utilization of Marine Biological Resources, Ministry of Natural Resources, Xiamen, 361005, China.

^b Fujian Provincial Key Laboratory of Innovative Drug Target Research and State Key Laboratory of Cellular Stress Biology, School of Pharmaceutical Sciences, Xiamen University, Xiamen 361102, China.

E-mail: fangmj@xmu.edu.cn; xu_yangj@xmu.edu.cn

Abstract

In this work, three series of ω -3 polyunsaturated fatty acid-alkanolamine derivatives (PUFA-AAs) were synthesized, characterized and their anti-inflammatory activity *in vivo* was evaluated. Compounds **4a**, **4f**, and **4k** exhibited marked anti-inflammatory activity in LPS-stimulated RAW 264.7 cells. The most promising compound **4k** dose-dependently suppressed the cytokines with IC_{50} values in the low micromolar range. Further, **4k** exhibited potential *in vitro* Nur77-binding affinity ($K_d = 6.99 \times 10^{-6}$ M) which is consistent with the result of docking studies. Next, the anti-inflammatory mechanism of **4k** was found to be through NF- κ B signal pathway in a Nur77-dependent manner. Moreover, we also observed **4k** significantly inhibited LPS-induced expression of cytokines (IL-6, TNF- α , and IL-1 β) through suppressing NF- κ B activation and attenuated LPS-induced inflammation in mouse acute lung injury (ALI) model. In conclusion, the study strongly suggests that the PUFA-AA derivatives can be particularly as new Nur77 mediators for further treatment in inflammatory diseases.

Keywords: Nur77; anti-inflammatory activity; ω -3 polyunsaturated fatty acid; molecular docking; acute lung injury.

Journal Pre-proofs

1. INTRODUCTION

Inflammation is the basic defense mechanism of the immune system, which can protect the body from harmful stimuli such as pathogens and toxins. Resolution of inflammation is necessary to re-establish homeostasis after injury or infection. Excessive inflammatory responses that fail to undergo resolution may lead to chronic inflammation associated with many diseases [1]. The critical role of inflammatory processes in health and disease has long been recognized, yet the detailed molecular mechanisms and biological events that regulate the progression and resolution of inflammation remain of interest. Acute inflammation in the body is less dangerous and can cause edema and intracellular flow due to changes in vascular permeability and local hemodynamics, whereas chronic inflammation can lead to diseases such as asthma, rheumatoid arthritis, and cancer [2]. In some cases, tumorigenesis and cancer progression are associated with inflammatory processes caused by pathogen infection [3]. Nonsteroidal anti-inflammatory drugs (NSAIDs) are important in the treatment of pain and inflammation, but long-term use of NSAIDs quickly leads to a high incidence of gastrointestinal adverse events [4]. Although many compounds have been found to possess anti-inflammatory activity [5-11], developing anti-inflammatory agents with the new structure and novel mechanism of action is still an urgent need.

Nur77 (also known as TR3, NGFIB, and NR4A1), as a member of the orphan nuclear receptor 4A (NR4A) subfamily, is an immediate-early response gene that plays a key role in hyper-cellular responses to multiple stimuli, such as mitogens, cytokines, stress, metabolic, and apoptotic signals [12-14]. Recent studies have highlighted the role of Nur77 as a significant regulator of the inflammatory response [15-19]. In human and mouse macrophages, inflammatory stimuli such as tumor necrosis factor- α (TNF- α), Toll-like receptor ligands, and lipopolysaccharide (LPS) can induce the expression of Nur77 which plays an important role in inflammatory responses [20, 21]. For example, the elevation of Nur77 expression was shown to lead to the reduction of expression of several cytokines and chemokines in macrophages in response to LPS or tumor necrosis factor stimulation [3]. In contrast, Nur77 deficiency elevated the production of inflammatory mediators, such as interleukin 1 beta (IL-1 β), interleukin-6 (IL-6), TNF- α , and nitric oxide (NO), in two mouse models of sepsis [22]. Several studies have

reported the molecular mechanisms of Nur77 mediating anti-inflammatory [3, 23]. A genomic analysis using *in vitro* modeling of monocyte adherence identified that Nur77 can attenuate the activation of the transcription factor nuclear factor κ B (NF- κ B) like I κ B α , an anti-inflammatory modulator [24]. NF- κ B is inactive in the cytoplasm of resting cells but it is activated and plays a critical role in inflammation [25]. Nur77 overexpression represses the activation of the inflammatory response in front of several stimuli, by preventing the NF- κ B interaction with its promoter [26]. Recently, it has been reported that Nur77 phosphorylation by p38 hampers its inhibition of NF- κ B in LPS-stimulated RAW264.7 cells, while PDNPA (*n*-pentyl 2-[3,5-dihydroxy-2-(1-nonanoyl)-phenyl]acetate) can impede the interaction between Nur77 and p38 α , prevent the p38 α phosphorylation of Nur77, and show strong anti-inflammatory [22]. Besides, the cross-talk between Nur77 and the inflammatory response can be mediated through other transrepression mechanisms. For instance, Nur77 overexpression inhibits NF- κ B nuclear translocation *via* the induction of I κ B α expression at the transcriptional level [27]. Also, it was demonstrated that the subcellular location of Nur77 from the nucleus to mitochondria was involved in Nur77-dependent anti-inflammatory inducing by celastrol and its analogs [28, 29]. Taken together, Nur77 is a potent therapeutic target for inflammatory disease and the discovery of anti-inflammatory inhibitors against Nur77 is an effective approach for the treatment of various inflammatory diseases.

Polyunsaturated fatty acids (PUFAs) are fatty acids containing two or more double bonds. PUFAs are classified as omega-3 (ω -3) and omega-6 (ω -6) based on the location of the last double bond relative to the terminal methyl end of the molecule. The ω -6/ ω -3 content of cell and organelle membranes and lipid membrane microdomains strongly influence membrane function and numerous cellular processes such as cell survival [30]. Nowadays, the importance of ω -3 PUFAs has been documented for many health benefits, not only resolving inflammation and prevention of infection, curing cancer, developing brain, also preventing cardiovascular disease (CVD) [31-33]. Published findings provide evidence suggested that ω -3 PUFAs might alleviate inflammatory diseases through several mechanisms, such as activation of G-protein-coupled receptor 110 (GPR110) [34], inhibition of the sterol regulatory element-binding protein (SREBP)

[35], plasma membrane remodeling of lymphocytes [36], oxygenation of endocannabinoids [31] and reduce lipid accumulation in adipose tissues [37]. Interestingly, a recent metabolomics study identified that PUFAs, including arachidonic acid (ARA) and docosahexaenoic acid (DHA), could bind to the ligand-binding domain (LBD) of the anti-inflammatory modulator Nur77, and Nur77-LBD might undergo conformational changes to mediate the small-molecule binding [38]. However, there is no literature at present of elucidating how PUFAs interact with Nur77-LBD. Besides, although the anti-inflammatory actions of PUFAs are well established, few studies have been conducted to evaluate the anti-inflammatory activity of PUFAs, especially the Nur77-dependent anti-inflammatory activity [39]. DHA, eicosapentaenoic acid (EPA), and docosapentaenoic acid (DPA) are the three major ω -3 PUFAs enriched in marine organisms, *e.g.* fish, shrimp, algae, and so on. Herein, we reported the synthesis and anti-inflammatory activities of a novel class of DHA/EPA/DPA derivatives that were created by covalently linking moieties alkanolamines to these ω -3 fatty acids (**Figure 1**). Furthermore, we evaluated the anti-inflammatory properties and *in vivo* ALI treatment effects of **4k**, one DPA derivative.

2. Result and Discussion

2.1. Chemistry

Design of the target compounds. **Figure 1** shows several potent binders of Nur77 and drug design conception of target compounds [22, 38, 40-42]. These potent binders of Nur77 including ARA and DHA have a hydrophilic head (blue) and a hydrophobic tail (black). DHA, EPA, and DPA, as three major ω -3 PUFAs, have many health benefits including resolving inflammation and prevention of infection. Besides, docosahexaenoyl ethanolamide (DHA-EA) was found endogenously in the human brain and retina, previous studies focus on cannabinoid receptor activation. Because they are multifunctional molecules, it is necessary to acknowledge that ω -3 PUFA-AAs could activate other receptors [43, 44]. Herein, in continuation to extend anti-inflammatory agents targeting Nur77, ω -3 PUFA-AA derivatives with the unsaturated fatty chains as the hydrophobic moiety and the hydroxyl group of alkanolamines as a hydrophilic head

were designed and screened for their anti-inflammatory activities in this study.

Insert Figure 1 here.

Figure 1. Several potent binders of Nur77 and drug design conception

Synthesis of the target compound. The synthetic procedure employed to obtain the target compounds **4a-4o** is depicted in Scheme 1. *cis*-4,7,10,13,16,19-Docosahexaenoic acid methyl ester (ω -3 DHA-ME, **1a**) and *cis*-7,10,13,16,19-docosapentaenoic acid methyl ester (ω -3 DPA-ME, **3a**) were prepared from the reactant of algae oil and methanol in the presence of alkali, while *cis*-5,8,11,14,17-eicosapentaenoic acid methyl ester (ω -3 EPA-ME, **2a**) from fish oil. The starting materials **1a/2a/3a** and ethanolamine/3-amino-1-propanol/4-amino-1-butanol/5-amino-1-pentanol/6-amino-1-hexanol were reacted in a free solvent at 80 °C for 24h to yield corresponding target compounds. All target compounds gave satisfactory analytical and spectroscopic data including ¹H NMR, ¹³C NMR, IR, and HRMS, which were in accordance with their depicted structures (**Scheme 1**).

Insert Scheme 1 here.

Scheme 1. General procedure for the synthesis of compounds **4a-4o**

2.2. Biological evaluation

2.2.1 Initial screening of target compounds against LPS-induced inflammation

The cytotoxic evaluation. The cytotoxicity of target compounds was evaluated in mouse RAW264.7 macrophages by the MTT assay to investigate the possible correlation between inflammatory inhibitory activity and cell viability. As shown in **Figure S1**, the relative cell viabilities of the treated cells were all more than 60% and

ten of the target compounds at 10 μ M showed no significant cytotoxicity in RAW264.7 cells. So target compounds at 10 μ M were further used to evaluate anti-inflammatory activity.

Initial Evaluation against LPS-induced NO production. Pro-inflammatory macrophages produce large amounts of NO, a molecule used to both attack pathogens and remodel intracellular metabolism [21]. To test whether our synthesized compounds inhibited the inflammatory mediator NO production, we used Griess reagent to detect the level of LPS-induced NO release in RAW264.7 cells treated with target compounds. The ability of the tested compounds to reduce pro-inflammatory cytokines NO was summarized in **Figure 2A**. LPS treatment caused a great increase of NO release compared to control, while compounds **4l**, **4m**, **4d**, **4n**, **4f**, **4a**, and **4k** could significantly alleviate the increase of LPS-induced NO release. Particularly, compounds **4a** and **4k** exhibited the most potent inhibitory activity and their NO inhibition rate was 83.33% and 84.92% at the concentration of 10 μ M, respectively.

Insert Figure 2 here.

Figure 2. *In-vitro* inhibition effect of synthesized compounds **4a-4o** against nitric oxide (A), TNF- α (B), IL-6 (C), and IL-1 β (D) productions induced by LPS in RAW 264.7 cells. RAW 264.7 cells were pretreated with or without compounds (10 μ M) for 2 h, and then cultured in the presence or absence of LPS (1 μ g/mL) for 24 h. The NO levels in the medium were determined by the Griess assay. The inflammatory genes expression of TNF- α , IL-6, and IL-1 β were determined by qPCR. The results were shown as means \pm SD (n = 3) of at least three independent experiments. #p < 0.05, ##p < 0.01, ###p < 0.001 compared with the control group; *p < 0.05, **p < 0.01, ***p < 0.001 compare with only LPS-stimulated group.

Initial Evaluation against LPS-Induced pro-inflammatory cytokine Release. TNF- α , IL-6, and IL-1 β are important pro-inflammatory mediators that play a crucial role in promoting the inflammatory process. Herein, the qPCR and Western Blot were used to

test the inhibitory effect of all synthetic compounds (**4a-4o**) on the mRNA and protein expressions of LPS-induced IL-1 β , TNF- α , and IL-6 in RAW 264.7 cells. Compounds **4a** and **4k** remarkably reduced the LPS-induced up-regulation of the mRNAs of these cytokines (**Figure 2B-2D**). Moreover, **4k** also significantly downregulated the protein expression of IL-1 β and TNF- α (**Figure 3**).

Insert Figure 3 here.

Figure 3. The suppression of synthesized compounds **4a-4o** on the protein expression of pro-inflammatory cytokines such as TNF- α and IL-1 β . RAW 264.7 mouse macrophages were pretreated with compounds (10 μ M) for 7.5 h, followed by incubation with LPS (1 μ g/mL) for 30 min. The cell lysates were subjected to immunoblotting assay for TNF- α , IL-1 β , and β -actin.

Initial SARs of PUFA-AA derivatives for the anti-inflammatory activity. The preliminary screening studies on anti-inflammatory activity indicated: (1) When ethanolamine (n=2) was introduced into PUFAs, there was a significant increase in anti-inflammatory activity. However, the increase in the number of carbon atoms in alkanolamine group led to an obvious decrease in anti-inflammatory activity, especially among DHA-AAs. We observed that **4a**, **4f**, and **4k** with ethanolamine moiety had the best anti-inflammatory activities among DHA-AAs, EPA-AAs, and DPA-AAs derivatives, respectively. (2) Except for **4a**, other DHA-AA derivatives showed lower anti-inflammatory activities than EPA-AA and DPA-AA derivatives, implying that $-(\text{CH}=\text{CH}-\text{CH}_2)_5-$ was better than $-(\text{CH}=\text{CH}-\text{CH}_2)_6-$ for anti-inflammatory activity. (3) Generally, among the three series of PUFA-AA derivatives, DPA-AA derivatives with 5 $-\text{CH}_2-$ at the carbon of the carboxyl group displayed the best inhibitory effect on the production of NO and pro-inflammatory cytokines in LPS-pretreated RAW 246.7 cells. It indicates that a long flexible linker between the polyallyl moiety and the carboxyl group of PUFA-AA is helpful for anti-inflammatory activity. To further explore SAR

information, we would like to perform the modification of the double bond of PUFA in future work.

Based on the results of initial screening, we found that compound **4k** at 10 μM showed superior inhibitory efficacies on all pro-inflammatory cytokine productions. Herein, compound **4k** was selected for further screening. As **4k** displayed slight toxic for macrophages with the cell growth inhibitory rate of 30.2%. We first examined the non-toxic concentrations of **4k** being used to evaluate anti-inflammatory activity. As shown in **S1B**, **4k** below 10 μM showed no significant cytotoxicity in RAW264.7 cells, and the relative cell viabilities of the dosing test cells exceeded 75% at 5 μM . Therefore, the non-toxic concentrations (5 μM , 2.5 μM , and 1.25 μM) were further used to evaluate the anti-inflammatory activity of **4k**.

2.2.2 Compound 4k dose-dependently inhibits the productions of pro-inflammatory cytokines

To confirm the anti-inflammatory effect of compound **4k**, the NO, TNF- α , and IL-6 levels in the medium were measured by ELISA assay and the mRNA and protein expression levels of pro-inflammatory cytokines in RAW264.7 cells were determined by qPCR and Western Blot, respectively. As shown in **Figure 4A-4C**, **4k** exhibited a dose-dependent inhibition of the LPS-induced releases of NO, TNF- α , and IL-6 at the concentrations ranging from 1.25 μM to 10 μM . Besides, compounds **4k** dose-dependently down-regulated the mRNA and protein expression levels of pro-inflammatory cytokines such as IL-1 β , IL-6, and TNF- α at the concentrations of 1.25, 2.5, 5, and 10 μM (**Figure 4D-4G**). These data indicate that **4k** may take excellent inhibitory effects on pro-inflammatory mediators and **4k** at 5 μM exhibited similar anti-inflammatory activity with the reference dexamethasone at 5 μM .

Insert Figure 4 here.

Figure 4. Compound **4k** dose-dependently inhibits NO, TNF- α , IL-6, and IL-1 β productions in LPS-stimulated RAW264.7 cells. (A) The NO levels in the medium. (B)

The TNF- α levels in medium. (C) The IL-6 levels in the medium. (D) The mRNA expression levels of IL-1 β in RAW264.7 cells. (E) The mRNA expression levels of IL-6 in RAW264.7 cells. (F) The protein expression levels of TNF- α and IL-1 β in RAW264.7 cells. RAW264.7 cells were plated for 24 h and then challenged with LPS (1 μ g/mL) with or without **4k** at different concentrations, NO levels in the medium were determined by the Griess assay and the levels of TNF- α and IL-6 levels in the medium were determined by ELISA. Besides, the mRNA expression levels of IL-1 β , and IL-6 and the protein expression levels of TNF- α and IL-1 β in RAW264.7 cells were determined by qPCR and Western Blot, respectively. Data are expressed as fold change relative to control values (samples treated with LPS alone), mean \pm SEM ($n \geq 3$). Student's t-test was used for the statistical analysis, # $p < 0.05$, ## $p < 0.01$, ### $p < 0.001$ compared with the control group; * $p < 0.05$ and ** $p < 0.01$ vs. LPS alone-stimulated group.

*2.2.3 Compound **4k** can bind to Nur77-LBD and take anti-inflammatory effects in a Nur77-dependent manner.*

4k binds to Nur77. In recent years, Nur77 has been confirmed as an important target for the development of anti-new inflammatory drugs [28]. Our prepared compounds have very similar structural features with several Nur77 binders previously reported. Compound **4k** exhibited good anti-inflammatory activity in LPS-treated RAW264.7. So, we used Surface Plasmon Resonance (SPR)-based assay and molecular docking study to evaluate the binding affinity of **4k** with Nur77-LBD. The SPR results showed that **4k** dose-dependently bound to Nur77-LBD with a K_d (equilibrium dissociation constant) value of 6.99×10^{-6} M, and exhibited slow association/dissociation kinetics to interact with Nur77-LBD (**Figure 5A**). To further understand how ω -3 PUFAs and their derivatives bind to Nur77-LBD, we performed molecular docking studies between the selected compounds (DHA, **4a**, and **4k**) and Nur77-LBD using induced-fit docking (IFD) program of Schrödinger software (Version 2019-1). The IFD docking scores of DHA, **4a**, and **4k** with Nur77-LBD (PDB: 4JGV) were -7.35, -4.50, and -9.40, respectively, while the native ligand THPN had an IFD docking score of -4.43 (**Table S1**). The

docking results indicated that ω -3 PUFAs and their derivatives had potential binding affinities with Nur77-LBD. The THPN-bound structure obtained using the IFD program was set as the reference for comparison. As depicted in **Figure 5B-5D**, **4k** bound to a region that overlapped with THPN binding region in the ligand-binding pocket of Nur77-LBD, the long fatty chains of **4k** and THPN were oriented in the same direction and produced hydrophobic interactions with the hydrophobic residues in the ligand-binding pocket. Besides, the alkanolamine moiety of **4k** was located in the same position as the 3,4,5-trihydroxyphenyl moiety of THPN. However, the alkanolamine moiety of **4k** formed two hydrogen bonds which interacted with the side chain hydroxyl group of residues THR513 (distance: 1.8 Å) and the backbone carbonyl oxygen of LEU509 (distance: 2.1 Å), while the 3,4,5-trihydroxyphenyl moiety of THPN only formed a hydrogen bond interaction with THR513 but no hydrogen bond interaction with LEU509. In addition, DHA and **4a** binding to Nur77 had similar conformation with THPN and **4k** (**Figure S2-S6**), but only **4k** formed an additional hydrogen-bond(s) with LEU509. Compared with the native ligand THPN ($\Delta G_{bind} = -49.89$ kcal/mol), DHA ($\Delta G_{bind} = -55.71$ kcal/mol), and **4a** ($\Delta G_{bind} = -55.31$ kcal/mol), **4k** ($\Delta G_{bind} = -99.51$ kcal/mol) showed a higher binding affinity to Nur77 (**Table S1**). These results might explain the better potency of **4k** compared to DHA and **4a** in the anti-inflammatory assay.

Insert Figure 5 here.

Figure 5. Compound **4k** binds to Nur77-LBD. (A) The physical binding affinity of **4k** to Nur77-LBD by SPR assay. (B) Comparison of THPN (blue) and **4k** (purple) binding to Nur77-LBD (PDB ID: 4JGV). (C) The IFD binding model of THPN in the ligand-binding pocket (LBP) of Nur77-LBD. (D) The IFD binding model of **4k** in the LBP of Nur77-LBD.

4k may suppress NF- κ B activity and take anti-inflammatory effects by targeting Nur77. It is well documented that Nur77 exerts an anti-inflammatory effect

through inhibiting NF- κ B activation in LPS-induced inflammation and NF- κ B activation is accompanied by phosphorylation and degradation of I κ B α [45]. Our above experiment results indicate that **4k** is both a good anti-inflammatory compound and a potent Nur77 ligand. However, the anti-inflammatory mechanism of **4k** remained elusive. Herein, in consideration of the subsequent *in vivo* anti-inflammatory assay, we first checked the levels of the pro-inflammatory cytokines (IL-1 β and TNF- α) and the key NF- κ B pathway-related proteins p-IKK α/β in human lung cancer H460 cells treated with or without **4k**. As shown in **Figure 6A**, the rise in the production of p-IKK α/β and pro-inflammatory molecules (IL-1 β and TNF- α) in LPS-treated H460 cells implied that LPS activated the NF- κ B pathway and induced inflammation, while **4k** could dose-dependently decrease p-IKK α/β , IL-1 β , and TNF- α , indicating that **4k** effectively inhibited NF- κ B activity and, as a result, dampened LPS-induced inflammation. To further confirm that the anti-inflammatory activity of **4k** was Nur77-related, we established Nur77 knockdown cells (Nur77 KD-H460 cells) through the transfection of Nur77 shRNA into H460 cells. The wild-type and Nur77-KD H460 cells were pretreated with LPS and then treated with or without **4k**, the levels of p-IKK α/β and I κ B α were then analyzed by Western Blot and visually represented by grayscale analysis (**Figure 6B**). It showed that LPS induced Nur77 expression both in wild and Nur77-KD H460 cells. It is consistent with previous studies. Meanwhile, we observed that p-IKK α/β had a significant decrease and I κ B α had a significant increase in LPS-stimulated wild H460 cells with **4k** pretreatment, indicating that **4k** inhibited NF- κ B activity. However, **4k** did not significantly change p-IKK α/β and I κ B α levels in the LPS-treated Nur77 KD-H460 cells. These data suggest that Nur77 is required for compound **4k** inhibition of LPS-induced macrophage cytokine and **4k** is a promising anti-inflammatory candidate for the treatment of inflammatory diseases.

Insert Figure 6 here.

Figure 6. Compound **4k** Nur77-dependently inhibits LPS-induced inflammation through NF- κ B signaling pathway in human normal lung H460 cells (A) Effects of compound **4k** on LPS-induced TNF- α , IL-1 β and p-IKK α/β protein expression in H460

cells. (B) The protein expression levels of I κ B α and p-IKK α / β in wild-type and Nur77^{-/-}-H460 cells treated with or without LPS and compound **4k**. Data are expressed as fold change relative to control values (samples treated with LPS alone), mean \pm SEM ($n \geq 3$). Student's t-test was used for the statistical analysis, # $p < 0.05$, ## $p < 0.01$, ### $p < 0.001$ compared with the control group; * $p < 0.05$ and ** $p < 0.01$ vs. LPS alone-stimulated group.

2.2.4 *In vivo* anti-inflammatory activity of **4k**

Acute inflammatory diseases remain the main cause of death in intensive care units worldwide. ALI is a critical illness that is primarily driven by inflammation [46-48]. Today, steroidal and nonsteroidal anti-inflammatory drugs are therapeutically limited in the treatment of ALI [49-51]. Besides, numerous pharmacological therapies for established ALI including corticosteroids and steroids have failed to show benefit in multicenter clinical trials. Therefore, today more and more researchers are focusing on the development of new agents for ALI treatment [52-54].

Importantly, recent studies have reported that Nur77 is involved in the pathogenesis of lung diseases including ALI and pulmonary fibrosis and Nur77 can be used as a therapeutic target for lung inflammation and diseases [23, 55, 56]. Besides, previous studies confirmed that ω -3 fatty acids had anti-inflammatory activity and could improve the clinical outcomes of patients undergoing ALI [57]. Interestingly, the Nur77-targeting compound **4k** could attenuate LPS-induced inflammation in wild human lung H460 cells [28]. Therefore, we induced ALI in mice by intratracheal LPS instillation to further evaluate *in vivo* anti-inflammatory activity of **4k**. Dexamethasone was used as a positive control, and DMSO was used as a vehicle. It was found that cytokines IL-6 and TNF- α in mice bronchial alveolar lavage fluid (BALF) had a marked increase after LPS instillation, while the increase was significantly inhibited by dexamethasone or **4k** treatment (**Figure 7A and 7B**). Besides, in LPS-induced lung tissues, I κ B α exhibited an increase with dexamethasone or **4k** pretreatment, accompanying with a decrease of TNF- α and IL-1 β (**Figure 7C**). These data suggested **4k** effectively attenuated pulmonary inflammation. Moreover, we performed

hematoxylin and eosin (H&E) staining of lung tissues to evaluate the protective effect of **4k** on ALI (**Figure 7D**). H&E staining showed the normal structure of lung tissue in control mice, without histopathologic changes under a light microscope. In the LPS group, the lung tissues exhibited marked pathologic changes, such as inflammatory infiltration, thickened alveolar septa, interstitial edema, and lung tissue destruction. These LPS-induced pathological changes were significantly reversed by treatment with **4k** or dexamethasone. Collectively, these results indicated that **4k** could potentially protect against pulmonary inflammation *in vivo*, and it could potentially be used for treating ALI and other inflammatory injuries.

Insert Figure 7 here.

Figure 7. Compound **4k** attenuates LPS-induced ALI in mice. (A) and (B) Concentrations of IL-6 and TNF- α were determined by ELISA assay in BALF samples. (C) Effects of compound **4k** on LPS-induced I κ B α , TNF- α , and IL-1 β protein expression in ALI lung tissue. Data were shown as mean \pm SEM, n = 6. #p < 0.05, ##p < 0.01, ###p < 0.001 compared with the control group; *p < 0.05, **p < 0.01, ***p < 0.001 vs LPS vehicle. (D) Hematoxylin and eosin (H&E) staining (Microscope magnification: 100*) showing reduced pathological changes in lung tissues from mice treated with **4k** compared to LPS challenged mice.

3. Conclusion

In summary, 15 PUFA-AA derivatives were synthesized as anti-inflammatory agents targeting Nur77. The *in vitro* anti-inflammatory activity was screened, the majority of PUFA-AA derivatives exhibited anti-inflammatory effects to different extents. The preliminary SAR studies show that the introduction of aminoethanol into polyunsaturated fatty acids (PUFAs) (e.g. **4a**, **4k**, and **4f**) could increase anti-inflammatory activity. Specifically, the most potent compound **4k** was selected to further study the mechanism. First, **4k** was found could dose-dependently suppress LPS-induced production of cytokines (TNF- α , IL-6, and IL-1 β) and inhibit NO production in RAW 246.7. Next, SPR assay and docking studies showed that **4k** had a

moderate binding affinity with Nur77. Moreover, we found **4k** significantly attenuated LPS-induced inflammation through the blocking of NF- κ B activation in a Nur77-dependent manner. Finally, *in vivo* studies in LPS-stimulated ALI mice showed that pretreatment with active compound **4k** led to a remarkable reduction of cytokines (IL-6, TNF- α , or IL-1 β) and I κ B α levels in BALF or lung tissues and pulmonary histopathological changes. Therefore, the Nur77-targeting compound **4k** is a promising potential anti-inflammatory candidate for the treatment of inflammatory diseases such as ALI.

4. Experimental section

Chemistry. Algae oil was purchased from Xiamen Kingdomway Group Company (Fujian, China). Other reagents were purchased and used without further purification unless otherwise indicated. The reactions were monitored by thin-layer chromatography (TLC). All NMR spectra were recorded on a Bruker 400 MHz NMR spectrometer, operating at 400 MHz for ^1H , and 100 MHz for ^{13}C , tetramethylsilane (TMS) was used as an internal reference for ^1H and ^{13}C chemical shifts, and DMSO- d_6 / CDCl_3 were used as the solvent. High-resolution mass spectra were determined on Micromass-LCT Premier Time of Flight (TOF) mass spectrometer (Waters, USA). HPLC was performed on Hanbon Nu3010C to collect different retention time for various target compounds. The infrared spectra were determined by A Bruker ALPHA Fourier-transform infrared (FTIR) spectrometer (Bruker Optics Inc., Germany).

Biology. MTT (3-(4,5-dimethylthiazol-2-yl)-2,5-diphenyltetrazolium bromide) was purchased from Beyotime (Beyotime, Shanghai, China). Lipopolysaccharide (LPS) was purchased from Sigma (Sigma, St. Louis, MO, USA). Standard molecules including EPA, DPA, and DHA were purchased from Tokyo Chemical Industry (TCI, Tokyo, Japan). Griess reagent was purchased from Beyotime (Beyotime, Shanghai, China). The mouse IL-6 enzyme-linked immunosorbent assay (ELISA) kit and mouse TNF- α ELISA kit were purchased from DAKWE (DAKWE, China). Trizol-reagent, the two-step M-MLV, and the Platinum SYBR Green qPCR SuperMix-UDG kit were purchased from YEASEN (YEASEN, Shanghai, China). I κ B α , IL-1 β , and TNF- α mAb

were purchased from Abcam (Abcam, Cambridge, UK), p-IKK α/β mAb was purchased from Cell Signaling Technology (CST, Boston, USA). Other reagents used in this study were purchased from the domestic market and were all analytically pure used without further purification. The absorbance of the cell samples for cell viability assay was measured in a microplate reader (Thermo Fisher Scientific, MA, USA). The relative RNA amounts were calculated with the $\Delta\Delta C_t$ method by Agilent AriaMx PCR (Agilent USA) instrument. BIAcore-T200 (GE, USA) was used to evaluate the binding affinity of **4k** with Nur77-LBD. The lung sections stained with hematoxylin and eosin were observed by light microscopy (Nikon, Japan).

4.2 Preparation of DHA- ME (**1a**), EPA- ME (**2a**), and DPA- ME (**3a**)

According to the slightly modified literature method, algae oil or fish oil (100 g) was dissolved in 125 mL methanol in a 250 mL round bottom flask equipped with a reflux condenser, then, 50 mL 20% NaOH (aq) was added to the mixture, and the reaction was stirred for 5 h at 75 °C. At the end of the reaction, the organic layer was separated and dried in vacuo [58]. The initial compounds **1a**, **2a**, and **3a** with the purity of >95% were obtained through the following process and directly used for the next reaction. First, **1a/3a** and **2a** were enriched by molecular distillation (1.0×10^{-3} mbar, 65 °C, the content of **1a/3a** increased from 37.08 to 75.59% and **2a** increased from 12.28 to 35.62%, respectively). Then, the product is purified by preparative HPLC (C18, methanol/H₂O = 90:10, t_R for **1a**, **2a**, **3a** was 10.2, 8.2, and 13.0 min, respectively). (**Scheme 1**)

4.3. General procedure for synthesis of the target compounds (**4a-4o**)

A mixture of **1a/2a/3a** (3 mmol) and ethanolamine/3-amino-1-propanol/4-amino-1-butanol/5-amino-1-pentanol/6-amino-1-hexanol (9 mmol) were added in 20 mL round bottom flask. The reaction mixture was stirred for 24 h at 80 °C, which was purified by silica gel column chromatography (petroleum ether/ethyl acetate 1:1) to give the target compounds (**4a-4o**) as pale yellow oil in yield of 57-78%. (**Scheme 1**)

cis-Docosa-4,7,10,13,16,19-hexaenoic acid (2-hydroxy-ethyl)-amide (4a). Pale yellow oil, yield 78%, HPLC purity: 98.3% ($t_R = 7.06$ min), ¹H NMR (400 MHz, DMSO-d₆, ppm): δ 7.76 (br, 1H, NH), 5.38-5.27 (m, 12H, 6 -CH=CH-), 4.61 (br, 1H,

OH), 3.40-3.32 (m, 2H, CH₂OH), 3.11-3.08 (m, 2H, NHCH₂), 2.83-2.77 (m, 10H, 5CH₂), 2.26-2.23 (m, 2H, CH₂), 2.13-1.99 (m, 4H, 2CH₂), 0.94-0.86 (m, 3H, CH₃). ¹³C NMR (100 MHz, DMSO-d₆, ppm): δ 172.00, 132.01, 129.42, 128.59, 128.56, 128.48, 128.37, 128.35, 128.32, 128.21, 128.16, 127.41, 60.44, 41.91, 35.63, 29.15, 25.68, 25.63, 25.58, 23.59, 20.50, 14.56. IR (KBr, cm⁻¹): ν̄ 3308 (N-H), 3028 (HC=CH), 1638 (C=O), 1548, 1406, 1268, 1069, 916, 668. HRMS (TOF-MS, +): *m/z* [M+H]⁺ calculated for C₂₄H₃₈NO₂⁺ 372.2897, found 372.2886.

***cis*-Docosa-4,7,10,13,16,19-hexaenoic acid (3-hydroxy-propyl)-amide (4b).** Pale yellow oil, yield 69%, HPLC purity: 95.4% (*t*_R = 7.14 min), ¹H NMR (400 MHz, DMSO-d₆, ppm): δ 7.73 (br, 1H, NH), 5.35-5.26 (m, 12H, 6 -CH=CH-), 4.37 (br, 1H, OH), 3.40-3.37 (m, 2H, CH₂OH), 3.08-3.04 (m, 2H, NHCH₂), 2.81-2.76 (m, 10H, 5CH₂), 2.26-2.21 (m, 2H, CH₂), 2.09-1.99 (m, 4H, 2CH₂), 1.54-1.48 (m, 2H, CH₂), 0.93-0.91 (m, 3H, CH₃). ¹³C NMR (100 MHz, DMSO-d₆, ppm): δ 171.84, 131.99, 129.36, 128.57, 128.53, 128.50, 128.35, 128.34, 128.30, 128.19, 128.15, 127.39, 58.86, 36.10, 35.68, 32.93, 25.66, 25.61, 25.56, 23.62, 20.48, 14.54. IR (KBr, cm⁻¹): ν̄ 3283 (N-H), 3011 (HC=CH), 1644 (C=O), 1532, 1447, 1069, 803, 729. HRMS (TOF-MS, +): *m/z* [M+H]⁺ calculated for C₂₅H₄₀NO₂⁺ 386.3054, found 386.3046.

***cis*-Docosa-4,7,10,13,16,19-hexaenoic acid (4-hydroxy-butyl)-amide (4c).** Pale yellow oil, yield 63%, HPLC purity: 98.4% (*t*_R = 6.95 min), ¹H NMR (400 MHz, DMSO-d₆, ppm): δ 7.72 (br, 1H, NH), 5.38-5.24 (m, 12H, 6 -CH=CH-), 4.34 (br, 1H, OH), 3.37-3.35 (m, 2H, CH₂OH), 3.01-3.00 (m, 2H, NHCH₂), 2.81-2.77 (m, 10H, 5CH₂), 2.26-2.21 (m, 2H, CH₂), 2.09-2.00 (m, 4H, 2CH₂), 1.39-1.37 (m, 4H, 2CH₂), 0.93-0.89 (m, 3H, CH₃). ¹³C NMR (100 MHz, DMSO-d₆, ppm): δ 171.61, 131.99, 129.39, 128.57, 128.54, 128.47, 128.35, 128.33, 128.30, 128.19, 128.14, 127.98, 127.39, 60.89, 38.81, 35.71, 30.37, 26.30, 25.66, 25.61, 25.56, 23.64, 20.48, 14.54. IR (KBr, cm⁻¹): ν̄ 3298 (N-H), 3012 (HC=CH), 1647 (C=O), 1549, 1445, 1268, 1062, 918, 712. HRMS (TOF-MS, +): *m/z* [M+H]⁺ calculated for C₂₆H₄₂NO₂⁺ 400.3210, found 400.3202.

***cis*-Docosa-4,7,10,13,16,19-hexaenoic acid (5-hydroxy-pentyl)-amide (4d).** Pale yellow oil, yield 67%, HPLC purity: 95.3% (*t*_R = 7.17 min), ¹H NMR (400 MHz,

DMSO-d₆, ppm): δ 7.72 (br, 1H, NH), 5.34-5.23 (m, 12H, 6 -CH=CH-), 4.32 (br, 1H, OH), 3.38-3.33 (m, 2H, CH₂OH), 3.02-2.97 (m, 2H, NHCH₂), 2.81-2.77 (m, 10H, 5CH₂), 2.21-2.23 (m, 2H, CH₂), 2.09-1.99 (m, 4H, 2CH₂), 1.42-1.32 (m, 4H, 2CH₂), 1.28-1.22 (m, 2H, CH₂), 0.93-0.89 (m, 3H, CH₃). ¹³C NMR (100 MHz, DMSO-d₆, ppm): δ 171.60, 131.99, 129.38, 129.06, 128.68, 128.56, 128.54, 128.47, 128.35, 128.32, 128.30, 128.17, 128.14, 127.39, 61.10, 38.85, 35.70, 32.68, 31.74, 29.53, 29.15, 25.66, 25.61, 25.56, 23.65, 23.42, 22.76, 22.53, 20.48, 14.54. IR (KBr, cm⁻¹): $\tilde{\nu}$ 3291 (N-H), 3010 (HC=CH), 1645 (C=O), 1541, 1450, 1265, 1060, 922, 749. HRMS (TOF-MS, +): m/z [M+H]⁺ calculated for C₂₇H₄₄NO₂⁺ 414.3367, found 414.3362.

cis-Docosa-4,7,10,13,16,19-hexaenoic acid (6-hydroxy-hexyl)-amide (4e). Pale yellow oil, yield 76%, HPLC purity: 95.5% (t_R = 7.38 min), ¹H NMR (400 MHz, DMSO-d₆, ppm): δ 7.72 (br, 1H, NH), 5.34-5.25 (m, 12H, 6 -CH=CH-), 4.31 (br, 1H, OH), 3.38-3.35 (m, 2H, CH₂OH), 3.01-2.97 (m, 2H, NHCH₂), 2.81-2.77 (m, 10H, 5CH₂), 2.26-2.21 (m, 2H, CH₂), 2.08-2.00 (m, 4H, 2CH₂), 1.40-1.35 (m, 4H, 2CH₂), 1.33-1.22 (m, 4H, 2CH₂), 0.93-0.89 (m, 3H, CH₃). ¹³C NMR (100 MHz, DMSO-d₆, ppm): δ 171.60, 131.99, 129.37, 128.56, 128.54, 128.47, 128.34, 128.32, 128.29, 128.17, 128.14, 127.39, 61.11, 38.87, 35.70, 32.95, 29.68, 26.79, 25.70, 25.65, 25.62, 25.56, 23.66, 20.48, 14.55. IR (KBr, cm⁻¹): $\tilde{\nu}$ 3305 (N-H), 3010 (HC=CH), 1612 (C=O), 1487, 1228, 1072, 750. HRMS (TOF-MS, +): m/z [M+H]⁺ calculated for C₂₈H₄₆NO₂⁺ 428.3523, found 428.3520.

cis-Eicosa-5,8,11,14,17-pentaenoic acid (2-hydroxy-ethyl)-amide (4f). Pale yellow oil, yield 70%, HPLC purity: 99.7% (t_R = 5.80 min), ¹H NMR (400 MHz, DMSO-d₆, ppm): δ 7.81 (br, 1H, NH), 5.36-5.31 (m, 10H, 5 -CH=CH-), 4.63 (br, 1H, OH), 3.38-3.35 (m, 2H, CH₂OH), 3.10-3.08 (m, 2H, NHCH₂), 2.83-2.78 (m, 6H, 3CH₂), 2.09-1.99 (m, 6H, 3CH₂), 1.54-1.43 (m, 4H, 2CH₂), 0.92-0.87 (m, 3H, CH₃). ¹³C NMR (100 MHz, DMSO-d₆, ppm): δ 172.47, 132.02, 130.09, 129.93, 128.59, 128.54, 128.44, 128.37, 128.33, 128.21, 128.16, 127.41, 60.46, 41.86, 35.83, 35.28, 31.59, 29.55, 29.48, 29.14, 27.06, 26.76, 25.73, 25.67, 25.58, 422.54, 20.50, 14.57. IR (KBr, cm⁻¹): $\tilde{\nu}$ 3297 (N-H), 3016 (HC=CH), 1645 (C=O), 1538, 1454, 1232, 10679, 972, 727. HRMS (TOF-MS, +): m/z [M+H]⁺ calculated for C₂₂H₃₆NO₂⁺ 346.2741, found 346.2735.

cis-Eicosa-5,8,11,14,17-pentaenoic acid (3-hydroxy-propyl)-amide (4g). Pale yellow oil, yield 57%, HPLC purity: 99.7% ($t_R = 5.90$ min), ^1H NMR (400 MHz, DMSO- d_6 , ppm): δ 7.75 (br, 1H, NH), 5.40-5.27 (m, 10H, 5 -CH=CH-), 4.42 (br, 1H, OH), 3.41-3.37 (m, 2H, CH_2OH), 3.10-3.05 (m, 2H, NHCH_2), 2.84-2.78 (m, 8H, 4 CH_2), 2.07-1.99 (m, 6H, 3 CH_2), 1.58-1.49 (m, 4H, 2 CH_2), 0.93-0.91 (m, 3H, CH_3). ^{13}C NMR (100 MHz, DMSO- d_6 , ppm): δ 172.34, 132.02, 129.91, 128.59, 128.52, 128.46, 128.37, 128.32, 128.22, 128.16, 127.41, 58.89, 36.08, 35.32, 32.96, 26.74, 25.79, 25.67, 25.58, 20.51, 14.58. IR (KBr, cm^{-1}): $\tilde{\nu}$ 3298 (N-H), 3011 (HC=CH), 1645 (C=O), 1546, 1445, 1263, 1070, 969, 711. HRMS (TOF-MS, +): m/z $[\text{M}+\text{H}]^+$ calculated for $\text{C}_{23}\text{H}_{38}\text{NO}_2^+$ 360.2897, found 360.2891.

cis-Eicosa-5,8,11,14,17-pentaenoic acid (4-hydroxy-butyl)-amide (4h). Pale yellow oil, yield 73%, HPLC purity: 99.6% ($t_R = 5.92$ min), ^1H NMR (400 MHz, CDCl_3 , ppm): δ 5.71 (br, 1H, NH), 5.45-5.32 (m, 10H, 5 -CH=CH-), 3.71-3.68 (m, 2H, CH_2OH), 3.33-3.28 (m, 2H, NHCH_2), 2.86-2.82 (m, 8H, 4 CH_2), 2.21-2.06 (m, 6H, 3 CH_2), 1.96 (br, 1H, OH), 1.77-1.69 (m, 2H, CH_2), 1.62-1.60 (m, 4H, 2 CH_2), 0.99-0.97 (m, 3H, CH_3). ^{13}C NMR (100 MHz, CDCl_3 , ppm): δ 173.06, 132.09, 129.16, 128.73, 128.61, 128.29, 128.24, 128.17, 128.09, 127.87, 127.00, 62.38, 39.20, 36.18, 29.67, 26.69, 26.34, 25.65, 25.57, 25.55, 20.57, 14.28. IR (KBr, cm^{-1}): $\tilde{\nu}$ 3298 (N-H), 3012 (HC=CH), 1646 (C=O), 1550, 1446, 1266, 1061, 920, 711. HRMS (TOF-MS, +): m/z $[\text{M}+\text{H}]^+$ calculated for $\text{C}_{24}\text{H}_{40}\text{NO}_2^+$ 374.3054, found 374.3045.

cis-Eicosa-5,8,11,14,17-pentaenoic acid (5-hydroxy-pentyl)-amide (4i). Pale yellow oil, yield 62%, HPLC purity: 95.1% ($t_R = 6.07$ min), ^1H NMR (400 MHz, CDCl_3 , ppm): δ 5.61 (br, 1H, NH), 5.43-5.34 (m, 10H, 5 -CH=CH-), 3.67-3.64 (m, 2H, CH_2OH), 3.29-3.24 (m, 2H, NHCH_2), 2.86-2.81 (m, 8H, 4 CH_2), 2.20-2.10 (m, 6H, 3 CH_2), 1.92 (br, 1H, OH), 1.74-1.70 (m, 2H, CH_2), 1.62-1.52 (m, 4H, 2 CH_2), 1.44-1.39 (m, 2H, CH_2), 0.99-0.97 (m, 3H, CH_3). ^{13}C NMR (100 MHz, CDCl_3 , ppm): δ 172.96, 132.08, 129.18, 128.71, 128.60, 128.29, 128.24, 128.16, 128.09, 127.86, 127.00, 62.54, 39.33, 36.17, 32.17, 29.70, 29.44, 26.69, 25.64, 25.57, 25.55, 23.04, 20.57, 14.28. IR (KBr, cm^{-1}): $\tilde{\nu}$ 3296 (N-H), 3012 (HC=CH), 1646 (C=O), 1550, 1447, 1261, 1060, 713. HRMS (TOF-MS, +): m/z $[\text{M}+\text{H}]^+$ calculated for $\text{C}_{25}\text{H}_{42}\text{NO}_2^+$ 388.3210, found

388.3203.

***cis*-Eicosa-5,8,11,14,17-pentaenoic acid (6-hydroxy-hexyl)-amide (4j).** Pale yellow oil, yield 73%, HPLC purity: 96.1% ($t_R = 7.41$ min), ^1H NMR (400 MHz, CDCl_3 , ppm): δ 5.54 (br, 1H, NH), 5.43-5.34 (m, 10H, 5 -CH=CH-), 3.66-3.63 (m, 2H, CH_2OH), 3.26-3.23 (m, 2H, NHCH_2), 2.87-2.81 (m, 8H, 4 CH_2), 2.19-2.07 (m, 6H, 3 CH_2), 1.83 (br, 1H, OH), 1.74-1.71 (m, 2H, CH_2), 1.59-1.50 (m, 4H, 2 CH_2), 1.41-1.35 (m, 4H, 2 CH_2), 0.99-0.97 (m, 3H, CH_3). ^{13}C NMR (100 MHz, CDCl_3 , ppm): δ 172.89, 132.08, 129.19, 128.71, 128.60, 128.29, 128.24, 128.16, 128.09, 127.86, 127.00, 62.63, 39.28, 36.18, 32.53, 29.67, 26.69, 26.49, 25.64, 25.58, 25.55, 25.27, 20.57, 14.28. IR (KBr, cm^{-1}): $\tilde{\nu}$ 3288 (N-H), 3010 (HC=CH), 1644 (C=O), 1542, 1451, 1262, 1060, 925, 749. HRMS (TOF-MS, +): m/z $[\text{M}+\text{H}]^+$ calculated for $\text{C}_{26}\text{H}_{44}\text{NO}_2^+$ 402.3367, found 402.3363.

***cis*-Docosa-7,10,13,16,19-pentaenoic acid (2-hydroxy-ethyl)-amide (4k).** Pale yellow oil, yield 65%, HPLC purity: 99.4% ($t_R = 8.31$ min), ^1H NMR (400 MHz, DMSO-d_6 , ppm): δ 6.21 (br, 1H, NH), 5.46-5.31 (m, 10H, 5 -CH=CH-), 3.72-3.70 (m, 2H, CH_2OH), 3.42-3.39 (m, 2H, NHCH_2), 2.85-2.82 (m, 6H, 3 CH_2), 2.81 (s, 1H, OH), 2.45-2.40 (m, 2H, CH_2), 2.30-2.26 (m, 2H, CH_2), 2.09-2.04 (m, 2H, CH_2), 1.40-1.26 (m, 8H, 2 CH_2), 0.90-0.88 (m, 3H, CH_3). ^{13}C NMR (100 MHz, DMSO-d_6 , ppm): δ 173.78, 130.52, 129.47, 128.63, 128.37, 128.06, 128.02, 127.99, 127.84, 127.53, 62.20, 42.40, 36.31, 31.51, 29.31, 27.22, 25.64, 25.60, 23.39, 22.57, 14.07. IR (KBr, cm^{-1}): $\tilde{\nu}$ 3295 (N-H), 3081 (HC=CH), 1646 (C=O), 1550, 1442, 1268, 1062, 710. HRMS (TOF-MS, +): m/z $[\text{M}+\text{H}]^+$ calculated for $\text{C}_{24}\text{H}_{40}\text{NO}_2^+$ 374.3054, found 374.3036.

***cis*-Docosa-7,10,13,16,19-pentaenoic acid (3-hydroxy-propyl)-amide (4l).** Pale yellow oil, yield 77%, HPLC purity: 96.3% ($t_R = 8.85$ min), ^1H NMR (400 MHz, DMSO-d_6 , ppm): δ 6.03 (br, 1H, NH), 5.40-5.39 (m, 10H, 5 -CH=CH-), 3.66-3.60 (m, 2H, CH_2OH), 3.44-3.40 (m, 2H, NHCH_2), 2.89-2.79 (m, 8H, 4 CH_2), 2.46-2.39 (m, 2H, CH_2), 2.31-2.27 (m, 2H, CH_2), 2.10-2.02 (m, 2H, CH_2), 1.97 (br, 1H, OH), 1.72-1.64 (m, 2H, CH_2), 1.41-1.25 (m, 6H, 3 CH_2), 0.92-0.90 (m, 3H, CH_3). ^{13}C NMR (100 MHz, DMSO-d_6 , ppm): δ 173.77, 130.52, 129.52, 128.63, 128.36, 128.04, 127.83, 127.52, 59.16, 36.40, 32.30, 31.51, 29.32, 27.24, 25.64, 23.45, 22.57, 14.09. IR (KBr, cm^{-1}): $\tilde{\nu}$

3298 (N-H), 3012 (HC=CH), 1645 (C=O), 1540, 1447, 1268, 1070, 750. HRMS (TOF-MS, +): m/z $[M+H]^+$ calculated for $C_{25}H_{42}NO_2^+$ 388.3210, found 388.3204.

***cis*-Docosa-7,10,13,16,19-pentaenoic acid (4-hydroxy-butyl)-amide (4m).** Pale yellow oil, yield 75%, HPLC purity: 98.5% (t_R = 8.38 min), 1H NMR (400 MHz, DMSO- d_6 , ppm): δ 5.75 (br, 1H, NH), 5.45-5.34 (m, 10H, 5 -CH=CH-), 3.71-3.68 (m, 2H, CH_2OH), 3.31-3.28 (m, 2H, $NHCH_2$), 2.86-2.81 (m, 8H, 4 CH_2), 2.43-2.40 (m, 2H, CH_2), 2.26-2.22 (m, 2H, CH_2), 2.10-2.06 (m, 2H, CH_2), 2.01 (br, 1H, OH), 1.63-1.60 (m, 4H, 2 CH_2), 1.39-1.27 (m, 6H, 3 CH_2), 0.92-0.89 (m, 3H, CH_3). ^{13}C NMR (100 MHz, DMSO- d_6 , ppm): δ 172.54, 130.53, 129.34, 128.63, 128.36, 128.33, 128.26, 128.05, 127.85, 127.53, 62.37, 39.24, 36.55, 31.52, 29.67, 29.33, 27.23, 26.31, 25.65, 25.62, 23.47, 22.58, 14.08. IR (KBr, cm^{-1}): $\tilde{\nu}$ 3287 (N-H), 3011 (HC=CH), 1645 (C=O), 1539, 1450, 1263, 1064, 925, 728. HRMS (TOF-MS, +): m/z $[M+H]^+$ calculated for $C_{26}H_{44}NO_2^+$ 402.3367, found 402.3361.

***cis*-Docosa-7,10,13,16,19-pentaenoic acid (5-hydroxy-pentyl)-amide (4n).** Pale yellow oil, yield 68%, HPLC purity: 98.0% (t_R = 8.69 min), 1H NMR (400 MHz, DMSO- d_6 , ppm): δ 5.71 (br, 1H, NH), 5.44-5.33 (m, 10H, 5 -CH=CH-), 3.66-3.61 (m, 2H, CH_2OH), 3.28-3.23 (m, 2H, $NHCH_2$), 2.98 (br, 1H, OH), 2.85-2.81 (m, 6H, 3 CH_2), 2.44-2.39 (m, 2H, CH_2), 2.25-2.21 (m, 2H, CH_2), 2.09-2.04 (m, 2H, CH_2), 1.61-1.50 (m, 8H, 4 CH_2), 1.44-1.31 (m, 6H, 3 CH_2), 0.91-0.88 (m, 3H, CH_3). ^{13}C NMR (100 MHz, DMSO- d_6 , ppm): δ 172.60, 130.52, 129.32, 128.62, 128.35, 128.32, 128.26, 128.04, 127.84, 127.52, 62.50, 39.39, 36.50, 32.12, 31.51, 29.36, 29.31, 27.22, 25.64, 25.61, 23.46, 23.02, 22.57, 14.07. IR (KBr, cm^{-1}): $\tilde{\nu}$ 3299 (N-H), 3011 (HC=CH), 1645 (C=O), 1547, 1448, 1264, 1180, 729. HRMS (TOF-MS, +): m/z $[M+H]^+$ calculated for $C_{27}H_{46}NO_2^+$ 416.3523, found 416.3519.

***cis*-Docosa-7,10,13,16,19-pentaenoic acid (6-hydroxy-hexyl)-amide (4o).** Pale yellow oil, yield 58%, HPLC purity: 97.8% (t_R = 9.04 min), 1H NMR (400 MHz, DMSO- d_6 , ppm): δ 5.57 (br, 1H, NH), 5.44-5.34 (m, 10H, 5 -CH=CH-), 3.66-3.63 (m, 2H, CH_2OH), 3.28-3.23 (m, 2H, $NHCH_2$), 2.86-2.81 (m, 8H, 4 CH_2), 2.45-2.39 (m, 2H, CH_2), 2.25-2.21 (m, 2H, CH_2), 2.10-2.04 (m, 2H, CH_2), 1.84 (br, 1H, OH), 1.59-1.50 (m, 4H, 2 CH_2), 1.43-1.29 (m, 10H, 5 CH_2), 0.92-0.88 (m, 3H, CH_3). ^{13}C NMR (100 MHz,

DMSO-d₆, ppm): δ 172.38, 130.52, 129.31, 128.62, 128.35, 128.31, 128.05, 127.84, 127.53, 62.64, 39.33, 36.55, 32.53, 31.52, 29.63, 29.32, 27.22, 26.50, 25.64, 25.62, 25.28, 23.48, 22.58, 14.08. IR (KBr, cm⁻¹): $\tilde{\nu}$ 3298 (N-H), 3009 (HC=CH), 1610 (C=O), 1585, 1263, 1076, 931, 752. HRMS (TOF-MS, +): m/z [M+H]⁺ calculated for C₂₈H₄₈NO₂⁺ 430.3680, found 430.3676.

4.4 Cell lines and cell culture

Mouse RAW 264.7 macrophages and Human large cell lung cancer cells (H460) were obtained from the American Type Culture Collection (ATCC, USA) and were incubated in DMEM media (Hyclone, Logan, Utah, USA) supplemented with 10% FBS, 100 U/mL penicillin, and 100 mg/mL streptomycin at 37 °C with 5% CO₂.

4.5 Cell viability assay

Cell cytotoxicity was evaluated by methyl thiazolyl tetrazolium (MTT) assay. Cells were inoculated at 4.5×10^3 cells per well in a 96-well plate. After cultured for 24 h, compounds at different concentrations were added into the cell culture medium in DMSO solution with the final concentration of DMSO is 0.1%, and the compound-treated cells were cultured for 24 h at 37 °C with 5% CO₂. Then 20 μ L of 5 mg/mL MTT reagent was added into the cells and incubated for 4 h. After 4 h, cell culture was removed and then 150 μ L DMSO was added to dissolve the formazan. The optical density was measured at 490 nm (OD₄₉₀). Cell viability was calculated from three independent experiments. The density of formazan formed in the blank group was set as 100% of viability.

$$\text{Cell viability (\%)} = \frac{\text{compound (OD}_{490})}{\text{blank (OD}_{490})} \times 100\%.$$

Blank: cultured with fresh medium only. Compound: treated with compounds or LPS.

4.6 Assay for NO production

RAW 264.7 cells were inoculated at 1×10^5 cells per well in a 24-well plate and cultured for 20 h. The cells were then pre-treated with different concentrations compounds which were prepared in a serum-free medium for 2 h before stimulation with LPS (1 μ g/mL). After LPS-stimulated for 24 h, the NO production was determined

by detecting the nitrite level using Griess reagent (Beyotime, Shanghai, China) according to the manufacturer's instructions, then measured absorbance of the samples at 570 nm (OD_{570}) in a microplate reader (Thermo Fisher Scientific, MA, USA).

4.7 Real-Time Quantitative PCR

RAW 264.7 cells were inoculated at 1×10^5 cells per well in a 24-well plate and cultured for 20 h. The cells were then pre-treated with different concentrations compounds which were prepared in a serum-free medium for 2 h before stimulation with LPS (1 $\mu\text{g}/\text{mL}$). After LPS-stimulated for 24 h, cells were homogenized in TRIZOL kit for extraction of RNA according to each manufacturer's protocol. Both reverse transcription and quantitative PCR were carried out using a two-step M-MLV Platinum SYBR Green qPCR SuperMix-UDG kit. (YEASEN, Shanghai, China) Eppendorf Mastercycler ep realplex detection system was used for qPCR analysis. The primers of genes including TNF- α , IL-6, IL-1 β , and GAPDH were synthesized by BAIJIN (BAIJIN, Xiamen, China). The primer sequences used are shown in Table 1. The amount of each gene was determined and normalized by the amount of GAPDH.

4.8 Western Blot Analysis

RAW264.7 cells were inoculated at 1×10^5 cells per well in a 24-well plate and cultured for 20 h. The cells were pretreated with different concentrations of different compounds for 7.5h, and then cultured in the presence or absence of LPS (1 $\mu\text{g}/\text{mL}$) for 0.5 h. After treatment, cells were washed with ice-cold PBS three times and lysed in RIPA buffer (Sangon, Shanghai, China). A Bradford protein assay was used to calculate the concentration of total protein in each sample. A routine Western blot operation was conducted to detect TNF- α (Abcam, Cambridge, UK), IL-1 β (Abcam, Cambridge, UK), p-IKK α/β (CST, Boston, USA), and I κ B α (Abcam, Cambridge, UK) expression, and normalized by the amount of β -actin or α -tubulin (CST, Boston, USA).

4.9 Determination of TNF- α and IL-6 in medium

RAW264.7 cells were inoculated at 1×10^5 cells per well in a 24-well plate and cultured for 20 h. The cells were then pre-treated with different concentrations compounds which were prepared in a serum-free medium for 2 h before stimulation

with LPS (1 $\mu\text{g}/\text{mL}$) for 24 h. After treatment of cells with compounds and LPS, the TNF- α and IL-6 levels in the medium were determined with an enzyme-linked immunosorbent assay (ELISA) kit (DAKEWE, China) according to the manufacturer's instructions. The total amount of the inflammatory factor in the media was normalized to the total protein quantity of the viable cell pellets.

4.10 Protein expression and purification

The human Nur77-LBD was cloned as an N-terminal histidine-tagged fusion protein in the pET15b expression vector and overproduced in *Escherichia coli* BL21 DE3 strain. Briefly, cells were harvested and sonicated, and the extract was incubated with the His60 Ni Superflow resin.

4.11 Surface Plasmon Resonance (SPR) Analysis

After coupling 5 μg purified ligand-binding domain (LBD) of Nur77 (Nur77-LBD) protein to CM5 of Biacore, compound **4k** (10 μM) with known anti-inflammatory activity were screened for its binding to Nur77-LBD by Biacore T200. The identified compound was tested again with a gradient concentration of 2.097 μM , 2.621 μM , 3.277 μM , 4.09 μM , 5.12 μM , 6.4 μM , 8.0 μM , and 10 μM injected through flow cells immobilized with Nur77-LBD. The binding kinetics between Nur77-LBD and compounds were analyzed at RT by Biacore T200. A CM5 sensor chip (GE Healthcare) was chemically activated by injecting 100 μL of N-ethyl-N0-3-(diethylaminopropyl) carbodiimide (EDC) (200 mM) and N-hydroxysuccinimide (NHS) (50 mM) (*v/v* 1:1). Purified Nur77-LBD dissolved in 10 mM sodium acetate (pH 4.5) and binding to the preactivated CM5 chip using amine coupling. The remaining ester groups were blocked by 1 M ethanolamine-HCl (pH 9.5). The amount of immobilized Nur77-LBD was detected by mass concentration dependent changes in the refractive index on the sensorchip surface, and corresponded to about 10,000 resonance units (RU). A serial concentration of compounds was added at a flow rate of 20 $\mu\text{L}/\text{min}$. When the data collection was finished in each cycle, the sensor surface was washed with glycine-HCl (10 mM, pH 2.5).

4.12 Molecular docking simulation

The molecular docking simulation was performed to better understand the binding mode of compound DHA, **4a**, and **4k** with Nur77. Molecular docking between selected compounds and Nur77-LBD was performed using Schrödinger software (Version 2019-1). The complex structure of Nur77-LBD (PDB ID: 4JGV) was used as a mode structure for molecular docking study. The protein prepared using the Protein Preparation Wizard of Schrödinger [59]. In this process, the force field applied OPLS3e and the root mean square deviation (RMSD) of the atom was specified as 0.30 Å, bond orders were assigned, unwanted waters were deleted and missing atoms were added. The selected compounds including DHA, **4a**, and **4k** were prepared using the LigPrep suit of Schrödinger with default settings and then bound to Nur77-LBD using the induced fit docking (IFD) protocol [60, 61]. To validate the docking method, the native ligand THPN was first re-docked to Nur77-LBD. The re-docking pose of THPN obtained using the IFD protocol had an RMSD of 1.0352 referring to the conformation of the crystal structure. The MM/GBSA (Prime MMGBSA v3.000) was used to calculate the absolute binding free energy of complexes from the docking result [62]. All of the docking studies were used the induced fit docking calculation protocol with default settings. Schrödinger's Maestro (Version 11.9) was used as the primary graphical user interface for the visualization of the crystal structure and docking results. The interaction analysis between molecule and protein complex employed by PyMol and the graphics of the binding site were generated using PyMol, version 2.3.0 (Open-Source PyMOL™ by Schrödinger) [63].

4.13 Mouse models

Male C57BL/6 mice of 20-25 g were obtained from the Animal Centre of Xiamen University (Xiamen, China). All animal care and experimental procedures were approved by the Animal Policy and Welfare Committee.

The LPS-induced ALI model [64, 65]. The ALI was induced in mice by intratracheal LPS instillation to evaluate the protective ability of **4k** against LPS-induced acute inflammation in vivo. mice were randomly divided into groups as follows: control (six mice received vehicle of 0.9% saline), LPS (six mice received LPS alone), dexamethasone, or **4k** (each of the two compounds was administered to a group of six

mice at 10 mg/kg, 20 mg/kg, 50 mg/kg). The active compounds were given daily *via* intraperitoneal injection consecutively for one week. The mice were euthanized with chloral hydrate 6 h after intratracheal injection of LPS at 6 mg/kg. Broncho alveolar lavage fluid (BALF), blood, and lung tissues were collected for further analysis.

4.14 Histopathologic examination of lung

The superior lobe of the right lung was collected and fixed in 4% paraformaldehyde, then embedded in paraffin and cut into 5 μ m sections. The sections were stained with hematoxylin and eosin using standard protocol for light microscopy examination.

4.15 Statistical Analysis.

All assays were performed in triplicate. The results were expressed as mean \pm SEM (standard deviation). Other data were analyzed by the SPSS statistical software, version 18.0 (SPSS Inc., USA). ANOVA with Tukey's post-test (One-way ANOVA for comparisons between groups) was used to compare values among different experimental groups using the GraphPad program. For experiments with only two groups, Student's t-test was used as specified in the figure legends. $p < 0.05$ was considered statistically significant (*), $p < 0.01$ as highly significant (**), $p < 0.001$ as extremely significant (***), and ns as not significant.

Conflicts of interest

There are no conflicts to declare.

Acknowledgments

This work was supported by grants from the Natural Science Foundation of Fujian Province of China (No. 2018J01132 and 2019J01011672), the Fundamental Research Funds for the Central Universities (No. 20720180051), and the Marine Economy Innovation Development Area Demonstration Project of Beihai (Bhsfs003, Bhsfs009).

References

- [1] I.M. Beck, W. Vanden Berghe, L. Vermeulen, K.R. Yamamoto, G. Haegeman, K. De Bosscher, Crosstalk in inflammation: the interplay of glucocorticoid receptor-based mechanisms and kinases and phosphatases, *Endocr Rev* 30(7) (2009) 830-882.
- [2] B.B. Finlay, G. McFadden, Anti-immunology: evasion of the host immune system by bacterial and viral pathogens, *Cell* 124(4) (2006) 767-782.
- [3] L. Zhao, H. Hu, J.A. Gustafsson, S. Zhou, Nuclear Receptors in Cancer Inflammation and Immunity, *Trends Immunol* 41(2) (2020) 172-185.
- [4] Y. Xie, M. Pan, Y. Gao, L. Zhang, W. Ge, P. Tang, Dose-dependent roles of aspirin and other non-steroidal anti-inflammatory drugs in abnormal bone remodeling and skeletal regeneration, *Cell Biosci* 9 (2019) 103.
- [5] N. Atatreh, A.M. Youssef, M.A. Ghattas, M. Al Sorkhy, S. Alrawashdeh, K.B. Al-Harbi, I.M. El-Ashmawy, T.I. Almundarij, A.A. Abdelghani, A.S. Abd-El-Aziz, Anti-inflammatory drug approach: Synthesis and biological evaluation of novel pyrazolo[3,4-d]pyrimidine compounds, *Bioorg Chem* 86 (2019) 393-400.
- [6] E.F. Lopes, F. Penteado, S. Thurow, M. Pinz, A.S. Reis, E.A. Wilhelm, C. Luchese, T. Barcellos, B. Dalberto, D. Alves, M.S. da Silva, E.J. Lenardao, Synthesis of Isoxazolines by the Electrophilic Chalcogenation of beta,gamma-Unsaturated Oximes: Fishing Novel Anti-Inflammatory Agents, *J Org Chem* 84(19) (2019) 12452-12462.
- [7] J. Dennis Bilavendran, A. Manikandan, P. Thangarasu, K. Sivakumar, Synthesis and discovery of pyrazolo-pyridine analogs as inflammation medications through pro- and anti-inflammatory cytokine and COX-2 inhibition assessments, *Bioorg Chem* 94 (2020) 103484.
- [8] S. Bua, L. Di Cesare Mannelli, D. Vullo, C. Ghelardini, G. Bartolucci, A. Scozzafava, C.T. Supuran, F. Carta, Design and Synthesis of Novel Nonsteroidal Anti-Inflammatory Drugs and Carbonic Anhydrase Inhibitors Hybrids (NSAIDs-CAIs) for the Treatment of Rheumatoid Arthritis, *J Med Chem* 60(3) (2017) 1159-1170.
- [9] W.A.A. Fadaly, Y. Elshaier, E.H.M. Hassanein, K.R.A. Abdellatif, New 1,2,4-triazole/pyrazole hybrids linked to oxime moiety as nitric oxide donor celecoxib analogs: Synthesis, cyclooxygenase inhibition anti-inflammatory, ulcerogenicity, anti-proliferative activities, apoptosis, molecular modeling and nitric oxide release studies, *Bioorg Chem* 98 (2020) 103752.
- [10] Q. Wang, H. Kuang, Y. Su, Y. Sun, J. Feng, R. Guo, K. Chan, Naturally derived anti-inflammatory compounds from Chinese medicinal plants, *J Ethnopharmacol* 146(1) (2013) 9-39.
- [11] S. Santhosh Kumar, A. Sajeli Begum, K. Hira, S. Niazi, B.R. Prashantha Kumar, H. Araya, Y. Fujimoto, Structure-based design and synthesis of new 4-methylcoumarin-based lignans as pro-inflammatory cytokines (TNF-alpha, IL-6 and IL-1beta) inhibitors, *Bioorg Chem* 89 (2019) 102991.
- [12] Y. Dai, W. Jin, L. Cheng, C. Yu, C. Chen, H. Ni, Nur77 is a promoting factor in traumatic brain injury-induced nerve cell apoptosis, *Biomed Pharmacother* 108 (2018) 774-782.
- [13] M. Liebmann, S. Hucke, K. Koch, M. Eschborn, J. Ghelman, A.I. Chasan, S. Glander, M. Schadlich, M. Kuhlencord, N.M. Daber, M. Eveslage, M. Beyer, M. Dietrich, P. Albrecht, M.

Stoll, K.B. Busch, H. Wiendl, J. Roth, I. Kuhlmann, L. Klotz, Nur77 serves as a molecular brake of the metabolic switch during T cell activation to restrict autoimmunity, *Proc Natl Acad Sci U S A* 115(34) (2018) E8017-E8026.

- [14] T.Y. Liu, X.Y. Yang, L.T. Zheng, G.H. Wang, X.C. Zhen, Activation of Nur77 in microglia attenuates proinflammatory mediators production and protects dopaminergic neurons from inflammation-induced cell death, *J Neurochem* 140(4) (2017) 589-604.
- [15] R. Rodriguez-Calvo, M. Tajés, M. Vazquez-Carrera, The NR4A subfamily of nuclear receptors: potential new therapeutic targets for the treatment of inflammatory diseases, *Expert Opin Ther Targets* 21(3) (2017) 291-304.
- [16] T.-Y.Y. Xiu-Ming Li, Xiao-Shun He, Jing-Ru Wang, Wen-Juan Gan, Shen Zhang, Jian-Ming Li, Hua Wu, Orphan nuclear receptor Nur77 inhibits poly (I:C)-triggered acute liver inflammation by inducing the ubiquitin-editing enzyme A20, *Oncotarget* 8(37) (2017) 61025-61035.
- [17] A.A. Hamers, C. Argmann, P.D. Moerland, D.S. Koenis, G. Marinkovic, M. Sokolovic, A.F. de Vos, C.J. de Vries, C.M. van Tiel, Nur77-deficiency in bone marrow-derived macrophages modulates inflammatory responses, extracellular matrix homeostasis, phagocytosis and tolerance, *BMC Genomics* 17 (2016) 162.
- [18] X.M. Li, X.X. Lu, Q. Xu, J.R. Wang, S. Zhang, P.D. Guo, J.M. Li, H. Wu, Nur77 deficiency leads to systemic inflammation in elderly mice, *J Inflamm (Lond)* 12 (2015) 40.
- [19] A. Kumar, T.M. Hill, L.E. Gordy, N. Suryadevara, L. Wu, A.I. Flyak, J.S. Bezbradica, L. Van Kaer, S. Joyce, Nur77 controls tolerance induction, terminal differentiation, and effector functions in semi-invariant natural killer T cells, *Proc Natl Acad Sci U S A* 117(29) (2020) 17156-17165.
- [20] L. Pei, A. Castrillo, M. Chen, A. Hoffmann, P. Tontonoz, Induction of NR4A orphan nuclear receptor expression in macrophages in response to inflammatory stimuli, *J Biol Chem* 280(32) (2005) 29256-29262.
- [21] D.S. Koenis, L. Medzikovic, P.B. van Loenen, M. van Weeghel, S. Huveneers, M. Vos, I.J. Evers-van Gogh, J. Van den Bossche, D. Speijer, Y. Kim, L. Wessels, N. Zelcer, W. Zwart, E. Kalkhoven, C.J. de Vries, Nuclear Receptor Nur77 Limits the Macrophage Inflammatory Response through Transcriptional Reprogramming of Mitochondrial Metabolism, *Cell Rep* 24(8) (2018) 2127-2140 e7.
- [22] L. Li, Y. Liu, H.Z. Chen, F.W. Li, J.F. Wu, H.K. Zhang, J.P. He, Y.Z. Xing, Y. Chen, W.J. Wang, X.Y. Tian, A.Z. Li, Q. Zhang, P.Q. Huang, J. Han, T. Lin, Q. Wu, Impeding the interaction between Nur77 and p38 reduces LPS-induced inflammation, *Nat Chem Biol* 11(5) (2015) 339-346.
- [23] A. Banno, S.P. Lakshmi, A.T. Reddy, S.C. Kim, R.C. Reddy, Key Functions and Therapeutic Prospects of Nur77 in Inflammation Related Lung Diseases, *Am J Pathol* 189(3) (2019) 482-491.
- [24] L. Diatchenko, S. Romanov, I. Malinina, J. Clarke, I. Tchivilev, X. Li, S.S. Makarov, Identification of novel mediators of NF-kappaB through genome-wide survey of monocyte adherence-induced genes, *J Leukoc Biol* 78(6) (2005) 1366-1377.

- [25] I. Lawrence, The nuclear factor NF-kappaB pathway in inflammation, *Cold Spring Harb Perspect Biol* 1(6) (2009) a001651.
- [26] H. Harant, I.J. Lindley, Negative cross-talk between the human orphan nuclear receptor Nur77/NAK-1/TR3 and nuclear factor-kappaB, *Nucleic Acids Res* 32(17) (2004) 5280-5290.
- [27] B. You, Y.Y. Jiang, S. Chen, G. Yan, J. Sun, The orphan nuclear receptor Nur77 suppresses endothelial cell activation through induction of IkappaBalpha expression, *Circ Res* 104(6) (2009) 742-749.
- [28] M. Hu, Q. Luo, G. Alitongbieke, S. Chong, C. Xu, L. Xie, X. Chen, D. Zhang, Y. Zhou, Z. Wang, X. Ye, L. Cai, F. Zhang, H. Chen, F. Jiang, H. Fang, S. Yang, J. Liu, M.T. Diaz-Meco, Y. Su, H. Zhou, J. Moscat, X. Lin, X.K. Zhang, Celastrol-Induced Nur77 Interaction with TRAF2 Alleviates Inflammation by Promoting Mitochondrial Ubiquitination and Autophagy, *Mol Cell* 66(1) (2017) 141-153 e6.
- [29] Z. Chen, D. Zhang, S. Yan, C. Hu, Z. Huang, Z. Li, S. Peng, X. Li, Y. Zhu, H. Yu, B. Lian, Q. Kang, M. Li, Z. Zeng, X.K. Zhang, Y. Su, SAR study of celastrol analogs targeting Nur77-mediated inflammatory pathway, *Eur J Med Chem* 177 (2019) 171-187.
- [30] J. Schumann, H. Fuhrmann, Impairment of NFkappaB activity by unsaturated fatty acids, *Int Immunopharmacol* 10(8) (2010) 978-984.
- [31] I. de Bus, R. Witkamp, H. Zuilhof, B. Albada, M. Balvers, The role of n-3 PUFA-derived fatty acid derivatives and their oxygenated metabolites in the modulation of inflammation, *Prostaglandins Other Lipid Mediat* 144 (2019) 106351.
- [32] P.C. Calder, Omega-3 fatty acids and inflammatory processes: from molecules to man, *Biochem Soc Trans* 45(5) (2017) 1105-1115.
- [33] B.N.Y. Setty, S.G. Betal, R.E. Miller, D.S. Brown, M. Meier, M. Cahill, N.B. Lerner, N. Apollonsky, M.J. Stuart, Relationship of Omega-3 fatty acids DHA and EPA with the inflammatory biomarker hs-CRP in children with sickle cell anemia, *Prostaglandins Leukot Essent Fatty Acids* 146 (2019) 11-18.
- [34] T. Park, H. Chen, H.Y. Kim, GPR110 (ADGRF1) mediates anti-inflammatory effects of N-docosahexaenoyl ethanolamine, *J Neuroinflammation* 16(1) (2019) 225.
- [35] R.K. Saini, Y.S. Keum, Omega-3 and omega-6 polyunsaturated fatty acids: Dietary sources, metabolism, and significance - A review, *Life Sci* 203 (2018) 255-267.
- [36] Y. Zhang, J. Min, L. Zhang, Anti-inflammatory and Immunomodulatory Effects of Marine n-3 Polyunsaturated Fatty Acids on Human Health and Diseases, *Journal of Ocean University of China* 18(2) (2019) 481-492.
- [37] N. Soni, A.B. Ross, N. Scheers, I. Nookaew, B.G. Gabrielson, A.S. Sandberg, The Omega-3 Fatty Acids EPA and DHA, as a Part of a Murine High-Fat Diet, Reduced Lipid Accumulation in Brown and White Adipose Tissues, *Int J Mol Sci* 20(23) (2019) 5895.
- [38] N. Vinayavekhin, A. Saghatelian, Discovery of a protein-metabolite interaction between unsaturated fatty acids and the nuclear receptor Nur77 using a metabolomics approach, *J Am Chem Soc* 133(43) (2011) 17168-17171.

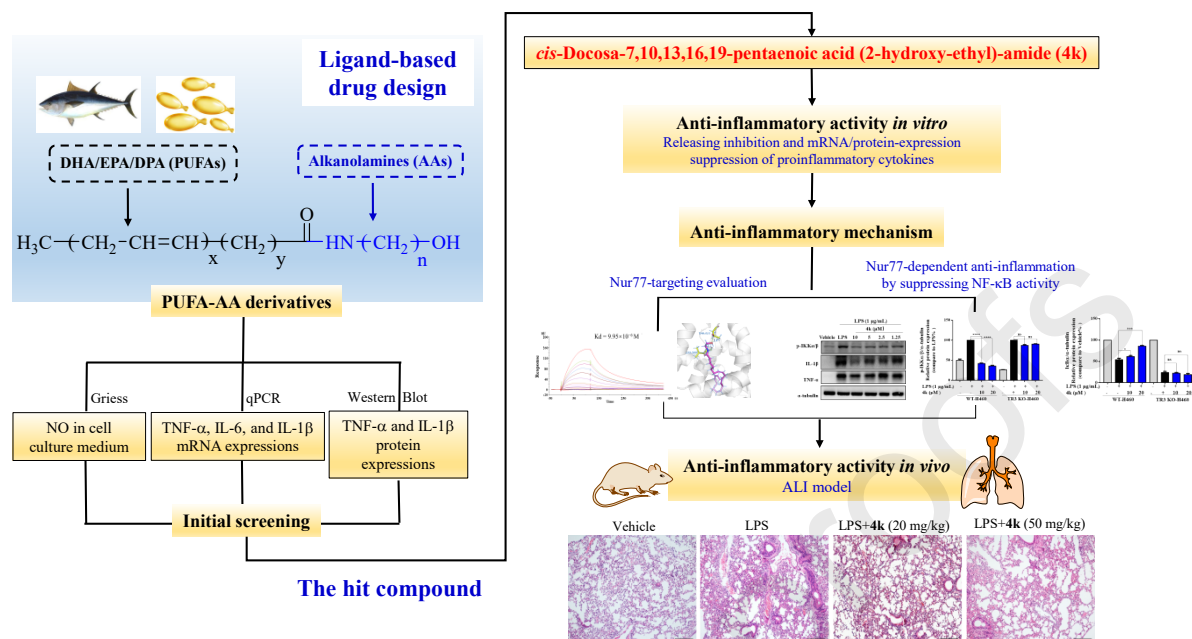
- [39] I.M. de Vera, P.K. Giri, P. Munoz-Iello, R. Brust, J. Fuhrmann, E. Matta-Camacho, J. Shang, S. Campbell, H.D. Wilson, J. Granados, W.J. Gardner, Jr., T.P. Creamer, L.A. Solt, D.J. Kojetin, Identification of a Binding Site for Unsaturated Fatty Acids in the Orphan Nuclear Receptor Nurrl, *ACS Chem Biol* 11(7) (2016) 1795-1799.
- [40] W.J. Wang, Y. Wang, H.Z. Chen, Y.Z. Xing, F.W. Li, Q. Zhang, B. Zhou, H.K. Zhang, J. Zhang, X.L. Bian, L. Li, Y. Liu, B.X. Zhao, Y. Chen, R. Wu, A.Z. Li, L.M. Yao, P. Chen, Y. Zhang, X.Y. Tian, F. Beermann, M. Wu, J. Han, P.Q. Huang, T. Lin, Q. Wu, Orphan nuclear receptor TR3 acts in autophagic cell death via mitochondrial signaling pathway, *Nat Chem Biol* 10(2) (2014) 133-140.
- [41] L. Pei, A. Castrillo, P. Tontonoz, Regulation of macrophage inflammatory gene expression by the orphan nuclear receptor Nur77, *Mol Endocrinol* 20(4) (2006) 786-794.
- [42] J.J. Liu, H.N. Zeng, L.R. Zhang, Y.Y. Zhan, Y. Chen, Y. Wang, J. Wang, S.H. Xiang, W.J. Liu, W.J. Wang, H.Z. Chen, Y.M. Shen, W.J. Su, P.Q. Huang, H.K. Zhang, Q. Wu, A unique pharmacophore for activation of the nuclear orphan receptor Nur77 in vivo and in vitro, *Cancer Res* 70(9) (2010) 3628-3637.
- [43] J.E. Watson, J.S. Kim, A. Das, Emerging class of omega-3 fatty acid endocannabinoids & their derivatives, *Prostaglandins Other Lipid Mediat* 143 (2019) 106337.
- [44] J. Roy, J.E. Watson, I.S. Hong, T.M. Fan, A. Das, Antitumorigenic Properties of Omega-3 Endocannabinoid Epoxides, *J Med Chem* 61(13) (2018) 5569-5579.
- [45] V.C. ei Chen, Xianglin Shi, and Laurence M. Demers, New Insights into the Role of Nuclear Factor- κ B, a Ubiquitous Transcription Factor in the Initiation of Diseases, *Clinical Chemistry* 45(1) (1999) 7-17.
- [46] R.B. Goodman, J. Pugin, J.S. Lee, M.A. Matthay, Cytokine-mediated inflammation in acute lung injury, *Cytokine & Growth Factor Reviews* 14(6) (2003) 523-535.
- [47] N.T. Mowery, W.T.H. Terzian, A.C. Nelson, Acute lung injury, *Curr Probl Surg* 57(5) (2020) 100777.
- [48] K. Tsushima, L.S. King, N.R. Aggarwal, A. De Gorordo, F.R. D'Alessio, K. Kubo, Acute lung injury review, *Intern Med* 48(9) (2009) 621-630.
- [49] D. Mokra, P. Mikolka, P. Kosutova, J. Mokry, Corticosteroids in Acute Lung Injury: The Dilemma Continues, *Int J Mol Sci* 20 (2019) 4765.
- [50] B. Guo, Y. Bai, Y. Ma, C. Liu, S. Wang, R. Zhao, J. Dong, H.L. Ji, Preclinical and clinical studies of smoke-inhalation-induced acute lung injury: update on both pathogenesis and innovative therapy, *Ther Adv Respir Dis* 13 (2019) 1-11.
- [51] Z. Zhang, Dexmedetomidine For The Treatment Of Acute Lung Injury: A Fact Or Fiction?, *J Invest Surg* 33(6) (2020) 584-586.
- [52] Q. Xia, X. Bao, C. Sun, D. Wu, X. Rong, Z. Liu, Y. Gu, J. Zhou, G. Liang, Design, synthesis and biological evaluation of novel 2-sulfonylindoles as potential anti-inflammatory therapeutic agents for treatment of acute lung injury, *Eur J Med Chem* 160 (2018) 120-132.
- [53] B.S. Wang, X. Huang, L.Z. Chen, M.M. Liu, J.B. Shi, Design and synthesis of novel

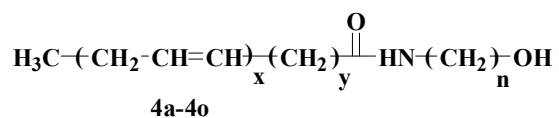
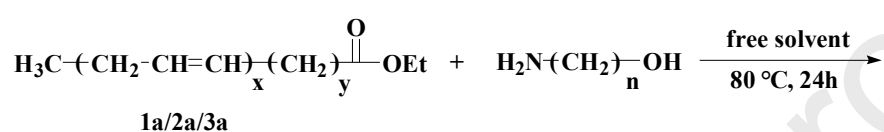
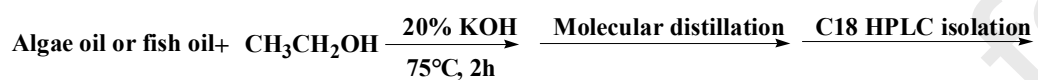
pyrazolo[4,3-d]pyrimidines as potential therapeutic agents for acute lung injury, *J Enzyme Inhib Med Chem* 34(1) (2019) 1121-1130.

- [54] Y. Hu, H. Yang, X. Ding, J. Liu, X. Wang, L. Hu, M. Liu, C. Zhang, Anti-inflammatory octahydroindolizine alkaloid enantiomers from *Dendrobium crepidatum*, *Bioorg Chem* 100 (2020) 103809.
- [55] K. Palumbo-Zerr, P. Zerr, A. Distler, J. Fliehr, R. Mancuso, J. Huang, D. Mielenz, M. Tomcik, B.G. Furnrohr, C. Scholtyssek, C. Dees, C. Beyer, G. Kronke, D. Metzger, O. Distler, G. Schett, J.H. Distler, Orphan nuclear receptor NR4A1 regulates transforming growth factor-beta signaling and fibrosis, *Nat Med* 21(2) (2015) 150-158.
- [56] K.D. Wansa, J.M. Harris, G. Yan, P. Ordentlich, G.E. Muscat, The AF-1 domain of the orphan nuclear receptor NOR-1 mediates trans-activation, coactivator recruitment, and activation by the purine anti-metabolite 6-mercaptopurine, *J Biol Chem* 278(27) (2003) 24776-90.
- [57] Z.Z. Ying Chen, Huanhuan Yang, Hongguo Lu, Effect of omega-3 fatty acids on acute lung injury and acute respiratory distress syndrome: a systematic review and meta-analysis, *Int J Clin Exp Med* 10(12) (2017) 15920-15926.
- [58] M. Li, T. Li, Enrichment of Omega-3 Polyunsaturated Fatty Acid Methyl Esters by Ionic Liquids Containing Silver Salts, *Separation Science and Technology* 43(8) (2008) 2072-2089.
- [59] G.M. Sastry, M. Adzhigirey, T. Day, R. Annabhimoju, W. Sherman, Protein and ligand preparation: parameters, protocols, and influence on virtual screening enrichments, *Journal of computer-aided molecular design* 27(3) (2013) 221-234.
- [60] W. Sherman, T. Day, M.P. Jacobson, R.A. Friesner, R. Farid, Novel procedure for modeling ligand/receptor induced fit effects, *Journal of medicinal chemistry* 49(2) (2006) 534-553.
- [61] R. Murphy, M. Repasky, Z. Zhou, R. Abel, G. Krilov, I. Tubert-Brohman, W. Sherman, R. Farid, R.A. Friesner, Evaluation of docking and scoring accuracy using a new version of Schrodinger's Glide XP and Induced Fit Docking (IFD) methodologies, ABSTRACTS OF PAPERS OF THE AMERICAN CHEMICAL SOCIETY, AMER CHEMICAL SOC 1155 16TH ST, NW, WASHINGTON, DC 20036 USA, 2011.
- [62] J.M. Swanson, R.H. Henchman, J.A. McCammon, Revisiting free energy calculations: a theoretical connection to MM/PBSA and direct calculation of the association free energy, *Biophysical journal* 86(1) (2004) 67-74.
- [63] W. DeLano, The PyMOL Molecular Graphics System. DeLano Scientific; San Carlos, CA, USA: 2002, 2002.
- [64] J. Qian, X. Chen, S. Shu, W. Zhang, B. Fang, X. Chen, Y. Zhao, Z. Liu, G. Liang, Design and synthesis novel di-carbonyl analogs of curcumin (DACs) act as potent anti-inflammatory agents against LPS-induced acute lung injury (ALI), *Eur J Med Chem* 167 (2019) 414-425.
- [65] G. Chen, B. Xiao, L. Chen, B. Bai, Y. Zhang, Z. Xu, L. Fu, Z. Liu, X. Li, Y. Zhao, G. Liang, Discovery of new MD2-targeted anti-inflammatory compounds for the treatment of sepsis and acute lung injury, *Eur J Med Chem* 139 (2017) 726-740.

Journal Pre-proofs

cis-Docosa-7,10,13,16,19-pentaenoic acid (2-hydroxy-ethyl)-amide (**4k**) acts as a Nur77 binder and exerts anti-inflammation by suppressing NF- κ B activity.





Where:

	x	y	Initial Compd.	n	Compd. No.
DHA-AA derivatives	6	2	1a	2/3/4/5/6	4a/4b/4c/4d/4e
EPA-AA derivatives	5	3	2a	2/3/4/5/6	4f/4g/4h/4i/4j
DPA-AA derivatives	5	5	3a	2/3/4/5/6	4k/4l/4m/4n/4o

Scheme 1. General procedure for the synthesis of compounds **4a-4o**

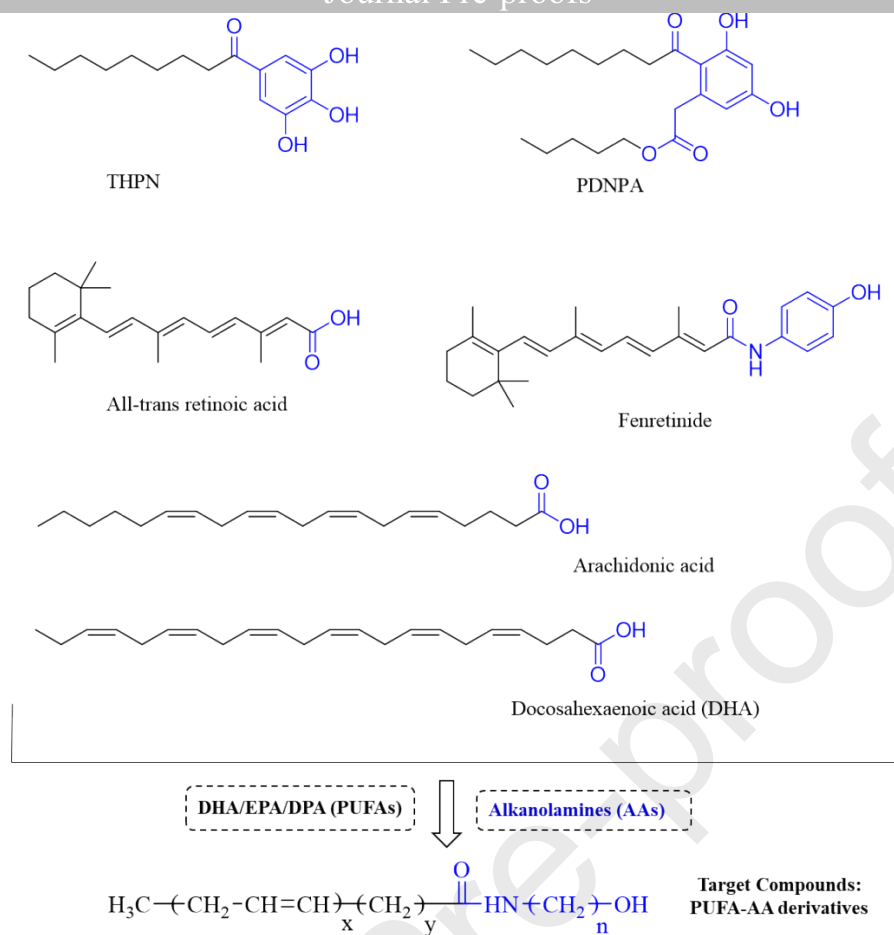


Figure 1. Several potent binders of Nur77 and drug design conception

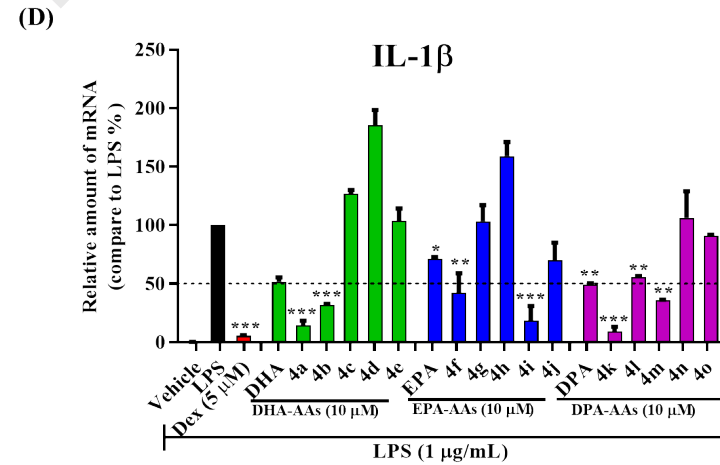
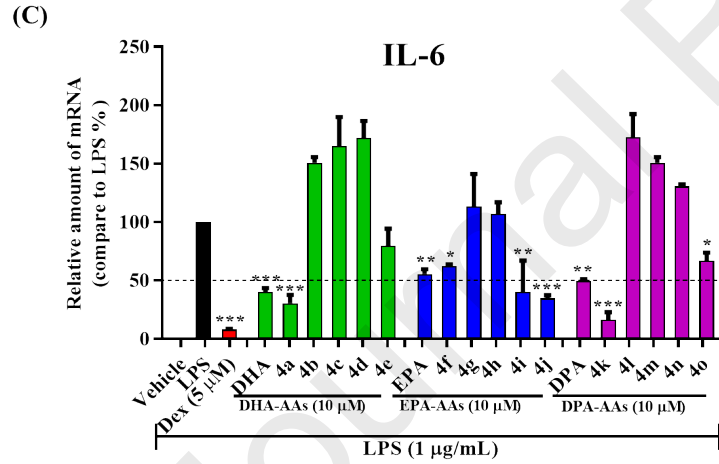
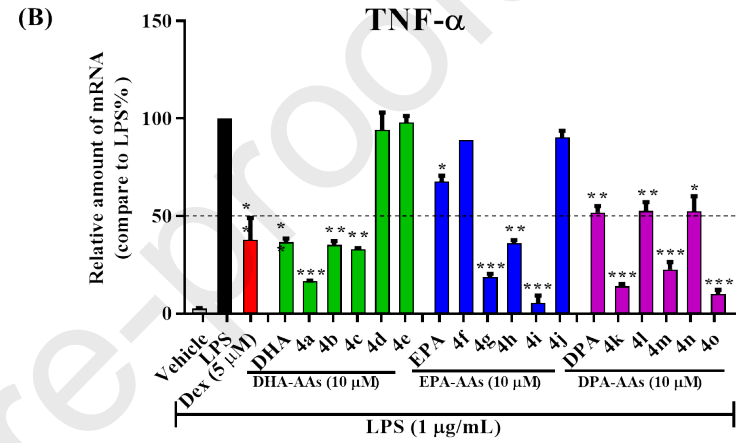
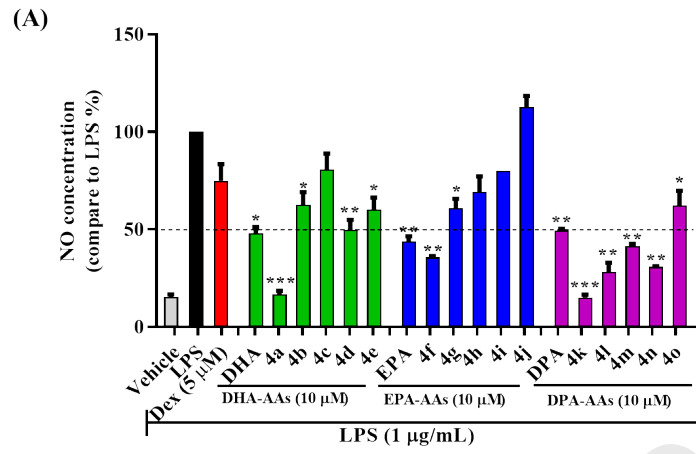


Figure 2. *In-vitro* inhibition effect of synthesized compounds **4a-4o** against nitric oxide (A), TNF- α (B), IL-6 (C), and IL-1 β (D) productions induced by LPS in RAW 264.7 cells. RAW 264.7 cells were pretreated with or without compounds (10 μ M) for 2 h, and then cultured in the presence or absence of LPS (1 μ g/mL) for 24 h. The NO levels in the medium were determined by the Griess assay. The inflammatory genes expression of TNF- α , IL-6, and IL-1 β were determined by qPCR. The results were shown as means \pm SD (n = 3) of at least three independent experiments. #p < 0.05, ##p < 0.01, ###p < 0.001 compared with the control group; *p < 0.05, **p < 0.01, ***p < 0.001 compare with only LPS-stimulated group.

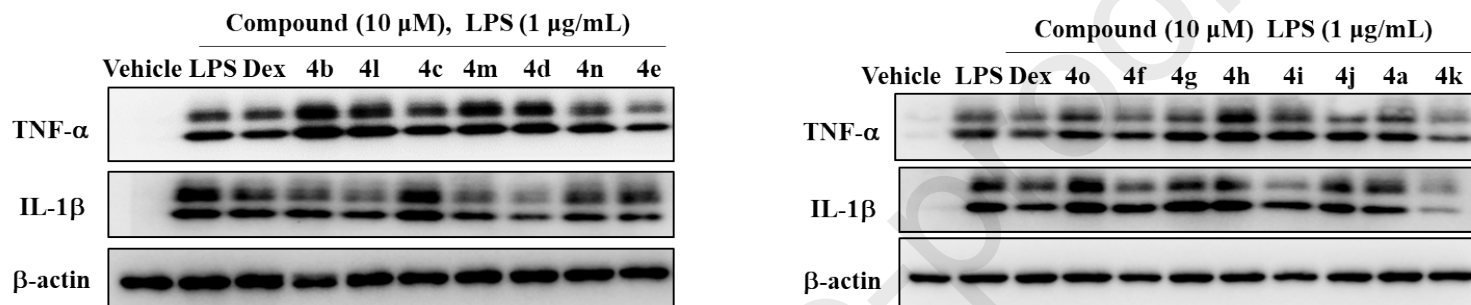


Figure 3. The suppression of synthesized compounds **4a-4o** on the protein expression of pro-inflammatory cytokines such as TNF- α and IL-1 β . RAW 264.7 mouse macrophages were pretreated with compounds (10 μ M) for 7.5 h, followed by incubation with LPS (1 μ g/mL) for 30 min. The cell lysates were subjected to immunoblotting assay for TNF- α , IL-1 β , and β -actin.

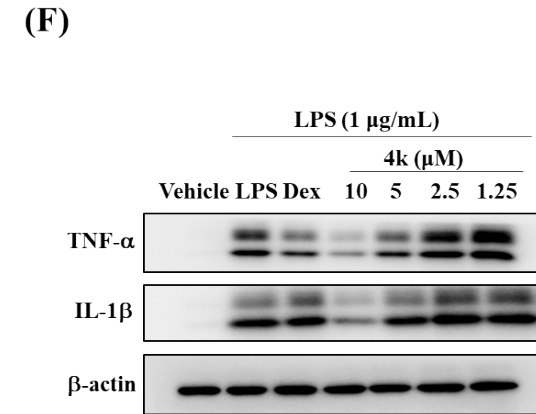
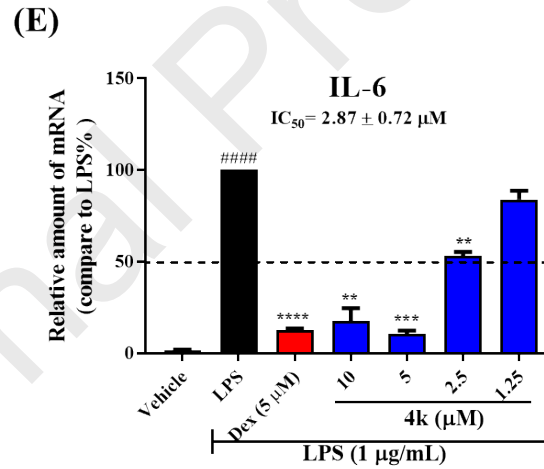
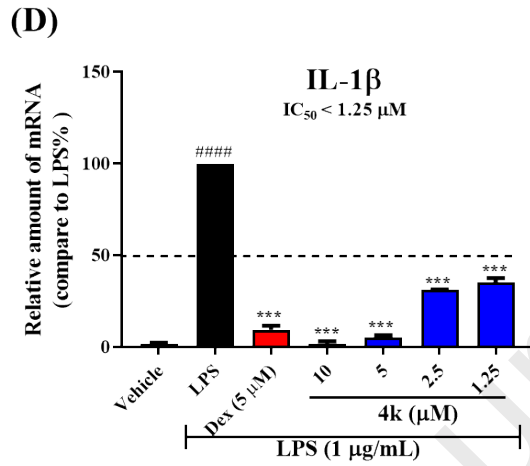
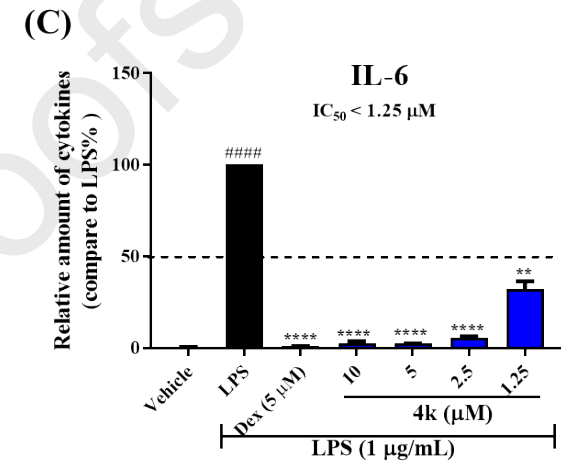
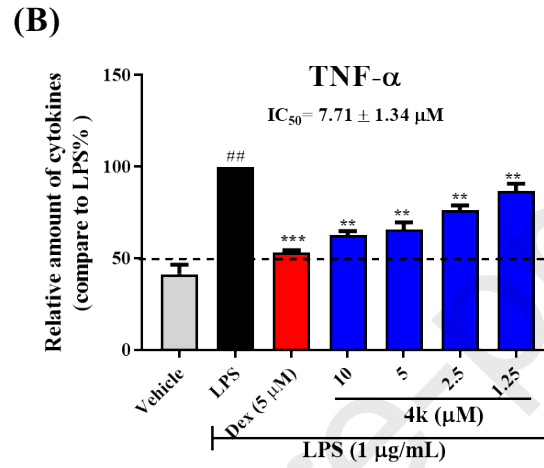
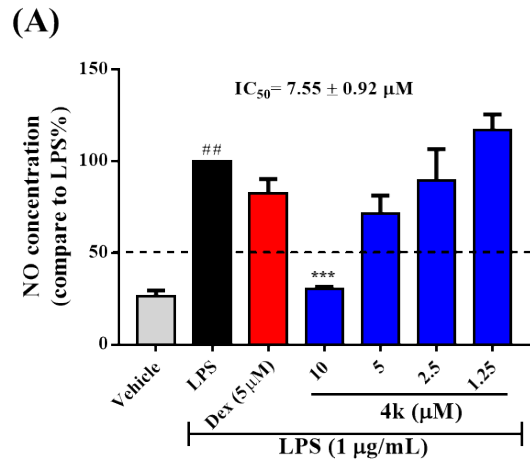


Figure 4. Compound **4k** dose-dependently inhibits NO, TNF- α , IL-6, and IL-1 β productions in LPS-stimulated RAW264.7 cells. (A) The NO levels in the medium. (B) The TNF- α levels in medium. (C) The IL-6 levels in the medium. (D) The mRNA expression levels of IL-1 β in RAW264.7 cells. (E) The mRNA expression levels of IL-6 in RAW264.7 cells. (F) The protein expression levels of TNF- α and IL-1 β in RAW264.7 cells. Macrophages were plated for 24 h and then challenged with LPS (1 μ g/mL) with or without **4k** at different concentrations, NO levels in the medium were determined by Griess and the levels of TNF- α and IL-6 levels in the medium were determined by ELISA. Besides, the mRNA expression levels of IL-1 β , and IL-6 and the protein expression levels of TNF- α and IL-1 β in RAW264.7 cells were determined by qPCR and Western Blot, respectively. Data are expressed as fold change relative to control values (samples treated with LPS alone), mean \pm SEM (n \geq 3). Student's t-test was used for the statistical analysis, #p < 0.05, ##p < 0.01, ###p < 0.001 compared with the control group; *p < 0.05 and **p < 0.01 vs. LPS alone-stimulated group.

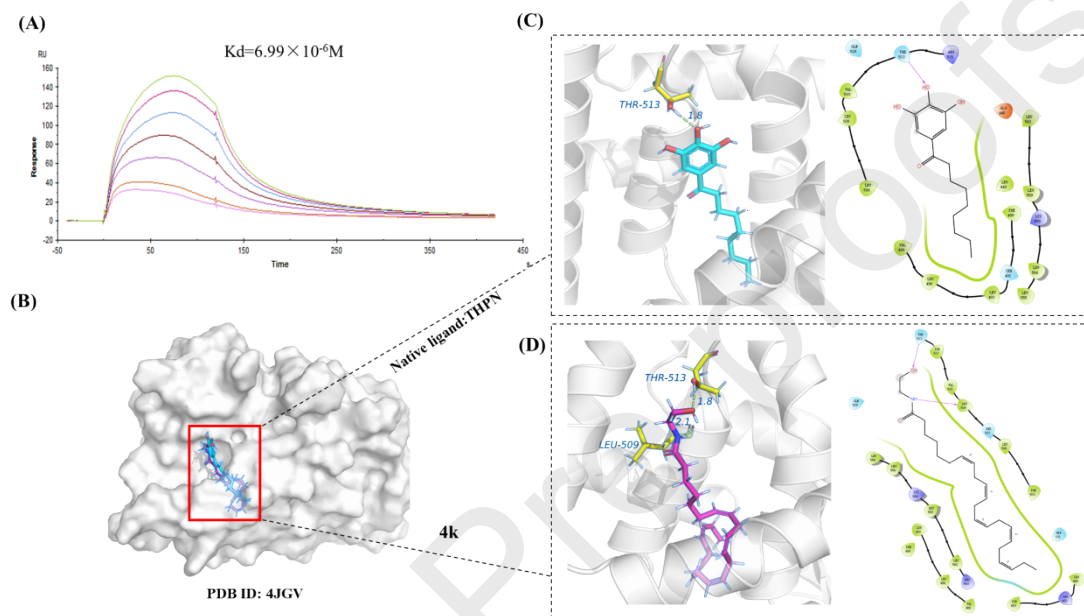


Figure 5. Compound **4k** binds to Nur77-LBD. (A) The physical binding affinity of **4k** to Nur77-LBD by SPR assay. (B) Comparison of THPN (cyan) and **4k** (magenta) binding to Nur77-LBD (PDB ID: 4JGV). (C) The IFD binding model of THPN in the ligand-binding pocket (LBP) of Nur77-LBD. (D) The IFD binding model of **4k** in the LBP of Nur77-LBD.

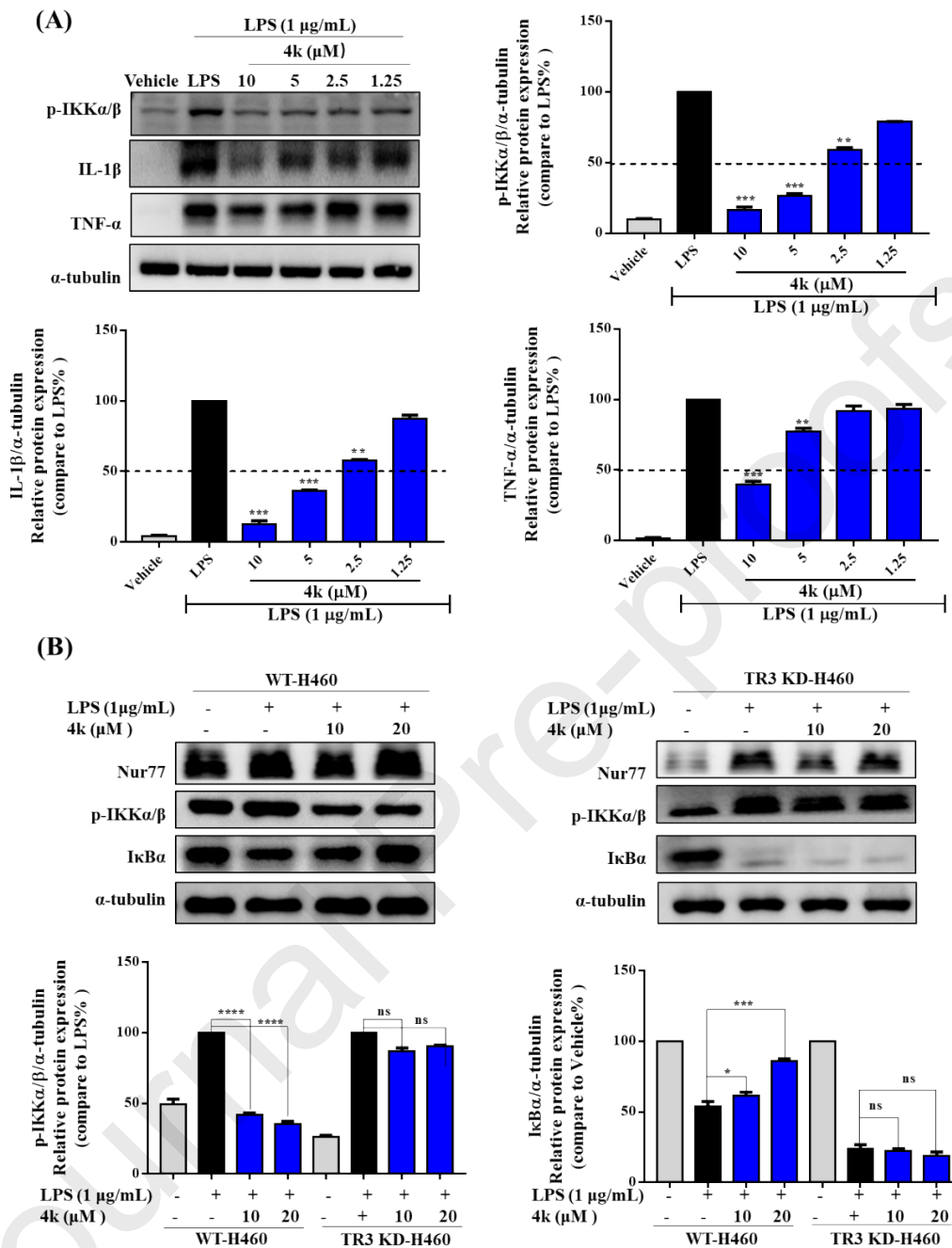


Figure 6. Compound **4k** Nur77-dependently inhibits LPS-induced inflammation through NF- κ B signaling pathway in human normal lung H460 cells (A) Effects of compound **4k** on LPS-induced TNF- α , IL-1 β and p-IKK α/β protein expression in H460 cells. (B) The protein expression levels of IkB α and p-IKK α/β in wild-type and Nur77 $^{-/-}$ -H460 cells treated with or without LPS and compound **4k**. Data are expressed as fold change relative to control values (samples treated with LPS alone), mean \pm SEM ($n \geq 3$). Student's t-test was used for the statistical analysis, # $p < 0.05$, ## $p < 0.01$, ### $p < 0.001$ compared with the control group; * $p < 0.05$ and ** $p < 0.01$ vs. LPS alone-stimulated group.

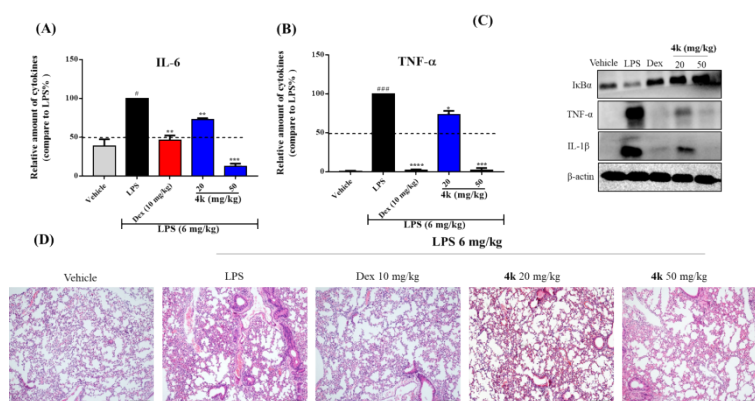


Figure 7. Compound **4k** attenuates LPS-induced ALI in mice. (A) and (B) Concentrations of IL-6 and TNF- α were determined by ELISA assay in BALF samples. (C) Effects of compound **4k** on LPS-induced I κ B α , TNF- α , and IL-1 β protein expression in ALI lung tissue. Data were shown as mean \pm SEM, $n = 6$. # $p < 0.05$, ## $p < 0.01$, ### $p < 0.001$ compared with the control group; * $p < 0.05$, ** $p < 0.01$, *** $p < 0.001$ vs LPS vehicle. (D) Hematoxylin and eosin (H&E) staining (Microscope magnification: 100 \times) showing reduced pathological changes in lung tissues from mice treated with **4k** compared to LPS challenged mice.

Synthesis and discovery of ω -3 polyunsaturated fatty acid-alkanolamine (PUFA-AA) derivatives as anti-inflammatory agents targeting Nur77

Hua Fang^{a,#}, Jianyu Zhang^{b,#}, Mingtao Ao^b, Fengming He^b, Weizhu Chen^a, Yuqing Qian^b, Yuxiang Zhang^b, Yang Xu^{b,*}, Meijuan Fang^{b,*}

Highlights:

- PUFA-AA derivatives **4a**, **4f**, and **4k** remarkably inhibit LPS-induced inflammation.
- **4k** dose-dependently exhibits anti-inflammatory activity *in vitro*.
- **4k** has a good binding affinity with Nur77-LBD.
- **4k** exerts a potent anti-inflammatory effect through the blocking of NF- κ B activation.
- **4k** displays the anti-inflammatory and protective effects on LPS-induced ALI in mice.